



Potential inhibitors of the enzyme acetylcholinesterase and juvenile hormone with insecticidal activity: study of the binding mode via docking and molecular dynamics simulations

Ryan S. Ramos, Williams J. C. Macêdo, Josivan S. Costa, Carlos H. T. de P. da Silva, Joaquín M. C. Rosa, Jorddy Neves da Cruz, Mozaniel S. de Oliveira, Eloisa H. de Aguiar Andrade, Raullyan B. L. e Silva, Raimundo N. P. Souto & Cleydson B. R. Santos

To cite this article: Ryan S. Ramos, Williams J. C. Macêdo, Josivan S. Costa, Carlos H. T. de P. da Silva, Joaquín M. C. Rosa, Jorddy Neves da Cruz, Mozaniel S. de Oliveira, Eloisa H. de Aguiar Andrade, Raullyan B. L. e Silva, Raimundo N. P. Souto & Cleydson B. R. Santos (2020) Potential inhibitors of the enzyme acetylcholinesterase and juvenile hormone with insecticidal activity: study of the binding mode via docking and molecular dynamics simulations, *Journal of Biomolecular Structure and Dynamics*, 38:16, 4687-4709, DOI: [10.1080/07391102.2019.1688192](https://doi.org/10.1080/07391102.2019.1688192)

To link to this article: <https://doi.org/10.1080/07391102.2019.1688192>



Published online: 11 Nov 2019.



Submit your article to this journal [↗](#)



Article views: 1037



View related articles [↗](#)



View Crossmark data [↗](#)



Citing articles: 30 View citing articles [↗](#)



Potential inhibitors of the enzyme acetylcholinesterase and juvenile hormone with insecticidal activity: study of the binding mode via docking and molecular dynamics simulations

Ryan S. Ramos^{a,b,c} , Williams J. C. Macêdo^{b,c}, Josivan S. Costa^{b,c}, Carlos H. T. de P. da Silva^d, Joaquín M. C. Rosa^e, Jorddy Neves da Cruz^f, Mozaniel S. de Oliveira^g, Eloisa H. de Aguiar Andrade^{f,h}, Raullyan B. L. e Silvaⁱ, Raimundo N. P. Souto^j and Cleudson B. R. Santos^{a,b}

^aGraduate Program in Biotechnology and Biodiversity-Network BIONORTE, Federal University of Amapá, Macapá, Brazil; ^bLaboratory of Modeling and Computational Chemistry, Department of Biological and Health Sciences, Federal University of Amapá, Macapá, Brazil; ^cLaboratory of Molecular Modeling and Simulation System, Federal Rural University of Amazônia, Capanema, Brazil; ^dComputational Laboratory of Pharmaceutical Chemistry, Faculty of Pharmaceutical Sciences of Ribeirão Preto, São Paulo, Brazil; ^eDepartment of Pharmaceutical Organic Chemistry, University of Granada, Granada, Spain; ^fAdolpho Ducke Laboratory, Emílio Goeldi Paraense Museum, Belém, Brazil; ^gProgram of Post-Graduation in Food Science and Technology, Federal University of Pará, Belém, Brazil; ^hProgram of Post-Graduation in Biodiversity and Biotechnology (BIONORTE), Federal University of Pará, Belém, Brazil; ⁱCenter of Biodiversity, Institute for Scientific and Technological Research of Amapá (IEPA), Brazil; ^jLaboratory of Arthropoda, Federal University of Amapá, Macapá, Brazil

Communicated by Ramaswamy H. Sarma

ABSTRACT

Models validation in QSAR, pharmacophore, docking and others can ensure the accuracy and reliability of future predictions in design and selection of molecules with biological activity. In this study, pyriproxyfen was used as a pivot/template to search the database of the Maybridge Database for potential inhibitors of the enzymes acetylcholinesterase and juvenile hormone as well. The initial virtual screening based on the 3D shape resulted in 2000 molecules with Tanimoto index ranging from 0.58 to 0.88. A new reclassification was performed on the overlapping of positive and negative charges, which resulted in 100 molecules with Tanimoto's electrostatic score ranging from 0.627 to 0.87. Using parameters related to absorption, distribution, metabolism and excretion and the pivot molecule, the molecules selected in the previous stage were evaluated regarding these criteria, and 21 were then selected. The pharmacokinetic and toxicological properties were considered and for 12 molecules, the DEREK software not fired any alert of toxicity, which were thus considered satisfactory for prediction of biological activity using the Web server PASS. In the molecular docking with insect acetylcholinesterase, the Maybridge3_002654 molecule had binding affinity of -11.1 kcal/mol, whereas in human acetylcholinesterase, the Maybridge4_001571 molecule show in silico affinity of -10.2 kcal/mol, and in the juvenile hormone, the molecule MCULE-8839595892 show in silico affinity value of -11.6 kcal/mol. Subsequent long-trajectory molecular dynamics studies indicated considerable stability of the novel molecules compared to the controls.

Abbreviations: QSAR: quantitative structure–activity relationships; PASS: prediction of activity spectra for substances

ARTICLE HISTORY

Received 4 June 2019
Accepted 23 October 2019

KEYWORDS

Validation; docking;
molecular dynamics;
Aedes aegypti

Introduction

Dengue virus (DENV) is a growing global health problem, annually, it is estimated that 390 million infections caused by DENV occur in tropical and subtropical areas around the world, of which approaching a quarter (~ 96 million) develop painful symptoms, debilitating disease with high fever, headache, malaise, rash, nausea, vomiting and joint/bone/muscle pain (Bardiot et al., 2018; Behnam, Graf, Bartenschlager, Zlotos, & Klein, 2015; Behnam, Nitsche, Boldescu, & Klein, 2016; Nitsche et al., 2013; Weigel, Nitsche, Graf, Bartenschlager, & Klein, 2015). The overall burden caused by DENV is considerable, as there are no antiviral drugs and vaccines available. A proportion of the cases ($\sim 500,000$)

progress to severe dengue, whose treatment is limited to symptomatic relief and supportive care, and an estimated 22,000 people succumb to DENV infections each year (Areiza, 2018; Costa et al., 2019; Hay et al., 2013; Kobayashi, Suzuki, Akahori, & Satoh, 2011; WHO, 2009).

DENV is transmitted by arthropod vectors, in particular mosquitoes such as *Aedes aegypti* and, to a lesser extent, *Aedes albopictus* and is therefore classified as an 'arbovirus' (virus transmitted by arthropods) (Leal et al., 2017; Osman, Idris, Kamarulzaman, Wahab, & Hassan, 2017; Sáez-Llorens et al., 2017). Vector control is the main preventive measure currently used to control dengue outbreaks. Vector mosquitoes are present in most subtropical regions but are

spreading to other regions due to urban growth, globalization and the inefficiency of chemical control. Dengue viruses persist in primates and humans in a 'wild' life cycle, from which the new serotypes may emerge in the future (Angel et al., 2017; Sittivicharpinyo, Wonnapijit, & Surat, 2017).

Attempts to develop dengue vaccines began about 90 years ago, but success so far has been limited. A major impediment to vaccination is that the vaccines should have a tetravalent effect, ie result in immunogenic response against the four serotypes of DENV. Vector chemical control of the is one of the main highlights in recent years, however, the mosquito has been adapting and creating resistance to these new insecticidal agents (Cavalcanti, Freitas, Brasil, & Cunha, 2017; Iswardy et al., 2017; Parvez & Parveen, 2017).

In the study of Ramos et al. (2019), the discovery of new inhibitors of insect/human acetylcholinesterase and juvenile hormone for *Aedes aegypti* was investigated with the aid of virtual screening, as the main mechanism of action for insecticidal activity involve inhibition of the acetylcholinesterase enzyme, sodium and potassium channel block, morphological developmental delay, octopamine site and gamma-aminobutyric acid (GABA) receptors.

There is currently no crystallographic structure of the enzyme acetylcholinesterase (AChE) for *Aedes aegypti* in the Protein Data Bank (PDB). However, studies by Kroupova, Ivařcu, Reimão-Pinto, Ameres, and Jinek (2019), showed that *D. melanogaster* AChE has 37%–39% amino acid sequence identity to the corresponding enzymes of *Anopheles gambiae* and *Ae. aegypti*, respectively; notably, the enzymes of *Ae. aegypti* and human acetylcholinesterase exhibit a slightly increased sequence identity of 48%–49% (Engdahl et al., 2015).

AChE is responsible for degradation of acetylcholine, a neurotransmitter which, when present in the synaptic cleft, promotes the propagation of the nerve impulse, since it causes the opening of sodium channels in the postsynaptic cell (Blenau, Rademacher, & Baumann, 2012). In the normal situation, after cessation of the stimulus, acetylcholine is removed by reuptake or by enzymatic degradation, with acetylcholinesterase being the enzyme responsible. Chemical agents act by inhibiting AChE, and consequently, acetylcholine remains in the synaptic cleft and the impulse does not cease, causing the insect to die.

Inhibition of juvenile hormone via the mechanism of action involves activity on target organ or molecule. In this case, they act hindering growth and development, interfering in cellular metabolism. Depending on the concentration used, some chemical agents may reduce the viability of eggs, nymphs, larvae and pupae. Reduction of egg numbers and inhibition of oviposition are important effects of plant extracts on insect reproduction.

Virtual screening (VS) is a valuable methodology for identifying potential therapeutic candidates and an alternative to the design of chemical compounds based on fragments or rational peptide design. VS has the benefit of being a high-throughput method and can be used to screen millions of chemical compounds, being more efficient and in terms of time and resources than screening for high-throughput

experimental methods, thanks to advances in computer hardware and algorithms related to drug design (Costa et al., 2018). In this study, virtual screening and molecular dynamics were used to identify new compounds capable of binding to insect/human acetylcholinesterase and juvenile hormone.

Materials and methods

Pivot/template compound

The bioactive conformation of the ligand pyriproxyfen was based on its crystallographic structure, according to Kang, Kim, Park, and Kim (2015) (CCDC reference: 1412612) and Ramos et al. (2019), and later used as starting point for the analysis of virtual screening by structural and electrostatic similarity in the ROCS and EON software.

Generation of conformers library in database

In this study, a commercial database was used to perform the virtual screening step: the Maybridge Database (<https://www.maybridge.com/>). Maybridge contains more than 53,000 organically produced compounds. The compounds are individually designed and produced by innovative synthetic techniques. This database is updated regularly and can be used for free on the webserver for download. For each molecule of the database, 300 conformers were generated using the MMFF94 force field implemented in the OMEGA software (Open Eye Scientific Software, Santa Fe, NM. <http://www.eyesopen.com>), in a computer with processor with Intel Core i7 2.4 GHz, using Windows 7 Professional operating system. The tension energy (energy difference between the actual conformer and the global minimum energy) was established to up to 9 kcal/mole, with a root mean square deviation (RMSD) of 0.6 Å (Hawkins & Nicholls, 2012) to generate non redundant conformers.

Virtual screening

Rapid overlay of chemical structures (ROCS)

Maybridge database was used to select molecules by virtual screening, in which the shape was approximated by Gaussians overlap in the central-atom and was used to calculate the maximum intersection of the volume of two molecules. In this study, the algorithm (Gaussian functions) implemented in the ROCS software (<https://www.eyesopen.com/rocs>) was used to generate and punctuate the three-dimensional database overlaps with the reference/template structure of pyriproxyfen and, thus, for obtaining 2000 top-ranked structures (Naylor et al., 2009; Silva et al., 2018).

Electrostatic similarity (EON)

Using the EON software (<https://www.eyesopen.com/eon>) the Tanimoto electrostatic index of the molecules selected in the database as well the structure of pyriproxyfen were calculated, in addition to calculations of partial charges for energy

minimization purposes (with the MMFF94 force field) (Naylor et al., 2009). The electrostatic classification was based on the electrostatic Tanimoto score, which varies from 1 (identical) to negative values, resulting from the overlapping of positive and negative charges. In this study, the lower energy conformer of pyriproxyfen was used for electrostatic comparison (more rigid conformation, based on available crystallographic structure). The output files were grouped according to the scores and the results were classified 'ET_combo' analogous to 'ComboTanimoto'. At the end, only the '100 major molecules/base' were selected.

In silico pharmacokinetic and toxicological properties

Molecules selected from the previous step were submitted to the QikProp software for obtaining pharmacokinetic properties. The parameters generated by the software allowed to select the candidate with a parameter of 95% approximation with pharmacokinetic characteristics of drugs already described in the literature, giving reliability to the data generated (Schrödinger, 2011; Yamashita et al., 2000). The parameters evaluated in the pharmacokinetic study were: number of property or descriptor values that fall outside the 95% range of similar values for known drugs (Star); predicted central nervous system activity (CNS), molecular weight (MW), predicted skin permeability (LogKp), estimated number of hydrogen bonds that would be donated by the solute to water molecules in an aqueous solution (HBD), estimated number of hydrogen bonds that would be accepted by the solute from water molecules in an aqueous solution (HBA), number of violations of Lipinski's rule of five (R5) and number of violations of Jorgensen's rule of three (R3).

The toxicity profile of the molecules was performed using DEREK software. DEREK is *in silico* toxicological prediction software used for drug design purposes (Lhasa Limited, 2007; Rindings, Barratt, & Cary, 1996; Sanderson & Earnshaw, 1991; Testa, Balmat, Long, & Judson, 2005).

Biological activity predictions of the compounds from virtual screening

Predictions of biological activity were performed using the Web server PASS, available at <http://www.pharmaexpert.ru/passonline> (Goel, Singh, Lagunin, & Poroikov, 2011). Using the PASS, it was possible to discover effects of a compound based entirely on the molecular formula using MNA (multi-level neighbors of atoms) descriptors, suggesting that the biological activity is in function of its chemical structure (Burkert & Allinger, 1982; Ferreira et al., 2017; Kirchmair et al., 2015). Only molecules with insecticidal and anticholinesterase activities were selected at this stage.

Molecular docking

In this step, only the top-ranked molecules with satisfactory results regarding to the pharmacokinetic, toxicological and biological activity predictions were selected for subsequent molecular docking simulations, in order to evaluate the energy

function score through the free binding energy (ΔG) of the ligands derived from the ligand-based virtual screening, as well as the analysis of the conformations, binding mode as well as binding affinity with the receptors here selected.

Selection of enzymes and inhibitors

Insecticides may act at different target sites (Braga & Valle, 2007), and two pathways of action mechanism were selected at this stage, related to acetylcholinesterase (AChE) and juvenile hormone (JH) receptor as well. AChE is a significant target because carbamates and organophosphates are classes of pesticides capable of inhibiting AChE. Thus, in spite of the high toxicity of these substances, they are still widely used in agriculture and domestic use and a high-resolution crystallographic structure of human AChE is already reported, isolated or in complex with inhibitor, thus justifying the use of this receptor in this step. Also, JH is a key regulator of insect development and breeding. In adult mosquitoes, it is essential for ovary maturation and normal male reproductive behaviour but is not clear how the distribution and activity of JH are regulated after secretion.

An additional comparative molecular modelling study was performed with the crystallographic structure of human acetylcholinesterase in complex with (–)-galantamine (GNT) in order to evaluate free energy, interactions with amino acid residues and binding affinity. The insect and human AChEs share high sequence similarity, according to data reported in literature (Blenau et al., 2012; Engdahl et al., 2015; Miyazawa, Tougo, & Ishihara, 2001; Ostettmann, Borloz, Urbain, & Marston, 2006; Savelev, Okello, Perry, Wilkins, & Perry, 2003). Thus, the lack of complex crystallographic structure of the acetylcholinesterase elucidated for *Aedes aegypti* was motivated by the choice of the targets here investigated.

The crystallographic structure of *Drosophila melanogaster* acetylcholinesterase (AChE) in complex with the tacrine derivative, 9-(3-iodobenzylamino)-1,2,3,4-tetrahydroacridine (I40), was downloaded from the Protein Data Bank (PDB) - PDB ID 1QON and resolution of 2.7 Å (Harel et al., 2000). The crystallographic structure of the recombinant human Acetylcholinesterase (AChE) in complex with (–) Galantamine (GNT), elucidated by X-ray diffraction, was downloaded from the Protein Data Bank (PDB) - PDB code 4EY6 and resolution of 2.4 Å (Cheung et al., 2012). The crystallographic structure of the juvenile hormone in complex with methyl (2E, 6E) -9 - [(2R) -3,3-dimethyloxiran-2-yl] -3,7-dimethylnona-2,6-dienoate, (JHIII), was downloaded - PDB code 5V13 and resolution of 1.87 Å (Kim et al., 2017). I40, GNT, JHIII and pyriproxyfen were used as positive control ligands in the molecular docking studies. Structures of the ligands complexed to acetylcholinesterase and juvenile hormone as well can be visualized in Figure 1.

Docking study using AutoDock 4.2/Vina 1.1.2 via graphical interface PyRx (v.0.8.30)

Ligands and structures of the proteins used in molecular docking studies were prepared using the Discovery Studio

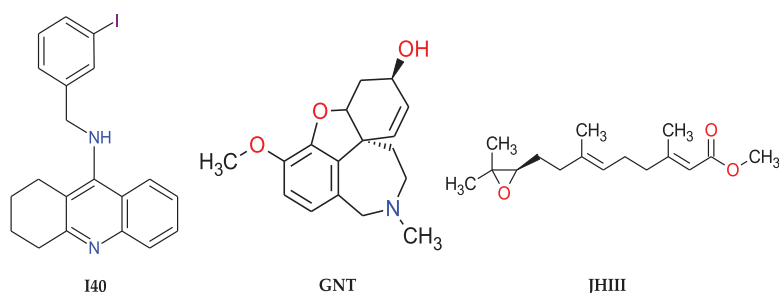


Figure 1. Structures of AChE inhibitors: 9-(3-iodobenzylamino)-1,2,3,4-tetrahydroacridine (I40), (-)-galanthamine (GNT) and methyl(2E,6E)-9-[(2R)-3,3-dimethoxyiran-2-yl]-3,7-dimethylnona-2,6-dienoate (JHIII).

5.0 software. The validation of the molecular docking of the ligand was performed by downloading the crystal structures of the proteins (PDB codes 1QON, 4EY6 and 5V13). In the docking study of AChE (from *D. melanogaster* as well as *Homo sapiens*) and juvenile hormone III (from *Aedes aegypti*), specific inhibitors were used with AutoDock 4.2/Vina 1.1.2 and PyRx v.0.8.30 (<https://pyrx.sourceforge.io>), respectively.

Molecular docking validation of the inhibitors were performed by comparing the crystallographic pose with the top-ranked docking conformation, based on the respective RMSD values (Budryn et al., 2015; Citro et al., 2016; Collado-González et al., 2017). Apart from Vina other docking software exists the LeadFinder (Martínez-Ballesta, DEL, Pérez-Sánchez, Moreno, & Carvajal, 2016), BINDSURF (Sánchez-Linares, Pérez-Sánchez, Cecilia, & García, 2012) and FlexScreen (Navarro-Fernández et al., 2012).

The *x*, *y*, and *z* coordinates of the receptors were determined according to the average region of the active site. The coordinates used for the centre of the grid can be seen in Table 1.

Toxicity risk assessment

ProTox, a virtual laboratory for predicting small molecule toxicities, as well as a useful tool to identify any undesirable toxic properties of our molecules were used (http://tox.charite.de/protox_II/) (Drwal, Banerjee, Dunkel, Wettig, & Preissner, 2014). Prediction was based on the similarity of the functional group of the query molecules with the *in vivo* reported and found in the software database. The toxic properties were determined as well as the LD50 values (in mg/kg), in addition to the toxicity class then classified.

Molecular dynamics (MD) procedures

We used the Restrained Electrostatic Potential (RESP) with HF/6-31G* basis set (Cornell, Cieplak, Bayly, & Kollman, 1993) to calculate the atomic charges of the inhibitors. These calculations were performed using the Gaussian 16 quantum chemistry software (Frisch et al., 2016). The parameters of the inhibitors were described by General Amber Force Field (GAFF) (Wang, Wolf, Caldwell, Kollman, & Case, 2004) and built using the Antechamber (Wang, Wang, Kollman, & Case, 2006). Amber 16 package was used for molecular dynamics simulations (Oliveira et al., 2019; Salomon-Ferrer, Case, & Walker, 2013). Proteins were treated with the ff14SB force

field (Maier et al., 2015) and the ionization state of their amino acids were studied with PROPKA server (Dolinsky, Nielsen, McCammon, & Baker, 2004), at neutral pH ($\cong 7$).

To describe the explicit water molecules, the TIP3P model was applied (Jorgensen, Chandrasekhar, Madura, Impey, & Klein, 1983). The partial charges of the protein–ligand complexes were neutralized by adding counter ions. All the complexes were immersed in an octahedral water box with periodontal conditions.

Energy minimization of the complexes was performed in four steps. Then, the systems were heated to 300K and finally, a DM simulation of 2 ns was performed to balance the systems. After all these steps, 100 ns of production DM simulation were performed.

We used the MPI sander for the four stages of energy minimization; in each of these stages, it took 3000 cycles using the steepest descent method and 5000 cycles using the conjugate gradient algorithm. In the first stage the hydrogen atoms of the water molecules, then the ions and the water molecules, were minimized in the third stage, the hydrogen atoms of the protein and in the last step the solute and the solvent underwent the process of energy minimization.

Three heating steps were used for a total time of 800 picoseconds to raise the system temperature to 300K. First, the solute was restricted with a constant harmonic force of $25 \text{ kcal mol}^{-1} \text{ \AA}^{-2}$, so only the solvent and the counter ions moved. In the next step the constant harmonic force was removed.

To balance the systems, we performed 2 ns simulations with no restriction at constant temperature. Finally, for each system, we performed 100 ns of molecular dynamics of production.

Particle Mesh Ewald method (Darden, York, & Pedersen, 1993) was used for the calculation of electrostatic interactions and the bonds involving hydrogen atoms were restricted with the SHAKE algorithm (Ryckaert, Ryckaert, Ciccotti, & Berendsen, 1977). Temperature control was performed with the Langevin thermostat (Izaguirre, Catarello, Wozniak, & Skeel, 2001) within collision frequency of 2 ps^{-1} .

Free energy calculations

Binding energies were estimated using the Molecular Mechanics-Generalized Born Surface Area (MM-GBSA) method (Cruz, Costa, Carvalho, & Alencar, 2019; Kollman

Table 1. Data from protocols here used for molecular docking validation purposes.

Enzyme	Inhibitor	Coordinates of the grid centre	Grid size (points)
AChE (PDB code: 1QON)	9-(3-Iodobenzylamino)-1,2,3,4-tetrahydroacridine	X = 33.4862 Y = 67.9151 Z = 9.4399	35 x 34 y 31 z
AChE (PDB code: 4EY6)	(-)-galanthamine	X = 9.090 Y = -60.485 Z = -23.703	32 x 38 y 36 z
Juvenile hormone (PDB code: 5V13)	methyl (2E,6E)-9-[(2R)-3,3-dimethyloxiran-2-yl]-3,7-dimethylnona-2,6-dienoate	X = -213.788 Y = 1.653 Z = 352.848	40 x 44 y 36 z

et al., 2000). The affinity energy calculation was used in 500 snapshots of the last 5 ns of the MD simulation trajectories. The free energy was calculated according to the following equations:

$$\Delta G_{\text{bind}} = \Delta H - T\Delta S \approx \Delta E_{\text{MM}} + \Delta G_{\text{solv}} - T\Delta S \quad (1)$$

where ΔG_{bind} is the free energy of the system resulting from the sum of the molecular mechanics energy (ΔE_{MM}), the desolvation free energy (ΔG_{solv}) and the entropy ($-T\Delta S$).

Energy of molecular gas phase mechanics (ΔE_{MM}) can be described by the sum of the internal energy contributions ($\Delta E_{\text{internal}}$), the sum of the connection, angle and dihedral energies, electrostatic contributions ($\Delta E_{\text{electrostatic}}$) and van der Waals terms (ΔE_{vdw}).

$$\Delta E_{\text{MM}} = \Delta E_{\text{internal}} + \Delta E_{\text{electrostatic}} + \Delta E_{\text{vdw}} \quad (2)$$

Solvation free energy (ΔG_{solv}) is the sum of the polar (ΔG_{GB}) and non-polar (ΔG_{nonpol}) contributions. The polar desolvation term was calculated using the implicit generalized born (GB) approaches.

$$\Delta G_{\text{solv}} = \Delta G_{\text{GB}} + \Delta G_{\text{nonpol}} \quad (3)$$

Per-residue free energy decomposition

Per-residue energy decomposition method (Gohlke, Kiel, & Case, 2003; Silva et al., 2019) was used to determine the chemical nature of the interactions of protein residues with inhibitors. Residual-inhibitory interaction energy can be described from four terms: van der Waals (ΔE_{vdw}) contribution and electrostatic (ΔE_{ele}) contribution in the gas phase, polar solvation (ΔG_{pol}) contribution, and nonpolar solvation (ΔG_{nonpol}) contribution, according to the equation:

$$\Delta G_{\text{inhibitor-residue}} = \Delta E_{\text{vdw}} + \Delta E_{\text{ele}} + \Delta G_{\text{pol}} + \Delta G_{\text{nonpol}} \quad (4)$$

Results and discussion

ROCS and EON

Starting point was the pyriproxyfen molecule here used as a pivot/template, which is a compound with average molar weight (321 Da), flexible and has a bioactive structure reported (Cheung et al., 2012; Ramos et al., 2019). Comparison between the three-dimensional (3D) shape of pyriproxyfen and the molecules found in the MayBridge library was performed via the Rapid Overlapping of Chemical Structures methodology (ROCS, version 2.1.1, OpenEye Scientific Software), in which the shape is approximated by

atom- and Gaussian functions and were used to calculate the maximum intersection of the volume of two molecules. The molecules selected using ROCS were classified by their shape Tanimoto index, which is a quantitative measure of three-dimensional overlap, in which 1 is equivalent to a complete overlap (same shape) and 0.5 is 50% overlap. The 2000 top-ranked molecules were selected considering a tanimoto index ranging from 0.580 to 0.880.

Considering electrostatic similarity (EON, version 1.1, OpenEye Scientific Software), a new reclassification was performed for the 2000 best ranked compounds (using ROCS and pyriproxyfen as a template). Electrostatic classification was based on an electrostatic Tanimoto index, which varies from one (identical) to negative, values resulting from the overlapping of positive and negative charges. The top 100 were chosen based on electrostatic scores ranging from 0.627 to 0.870.

Pharmacokinetic and toxicological properties

At this stage, the top 100 selected in the previous step followed for predictions of the pharmacokinetic properties that resulted in the selection of 21 molecules, which were compared with the *in silico* properties of the pivot compound, such as shown in Table 2. The 'star' parameter means the number of property values or descriptors that are outside the 95% interval of values reported for known drugs. A large number of 'star' suggests that a molecule has more violations and less drug-like characteristics than molecules with less 'star'.

Considering the established parameters of absorption, distribution, metabolism and excretion (Lipinski, Lombardo, Dominy, & Feeney, 2001) and the pivotal molecule, the molecules selected in the previous step were evaluated within these criteria, and 21 were then selected, in which they satisfy the required conditions (Gaddaguti, Rao, & Rao, 2016). All the molecules tested in this study exhibit hydrogen bonding and hydrophobic interactions with corresponding amino acids, according to molecular docking simulations. The template compound showed a skin permeability violation, and the same condition was also observed for 5 molecules, which can be exemplified by a high similarity between the molecules tested, thus corroborated by the studies carried out by Gaddaguti et al. (2016) and Ramos et al. (2019). Compounds with less or preferably no violations of these rules are more likely to be orally administered/available.

The toxicological properties of the molecules with toxicity alerts are shown in Table 3. It is noted that the pyriproxyfen

Table 2. Pharmacokinetic properties calculated for selected molecules.

Molecule	Star ^a	CNS ^b	PM ^c	logKp ^d	HBD ^e	HBA ^f	R5 ^g	R3 ^h
Normal range	0–5	–2 to +2	<500	–8 to –1	0–6	2–20	Max 4	Max 3
Pyriproxyfen	1	1	321.4	0.8	0	2.25	1	0
Maybridge3_005516	0	–1	319.4	–1.9	1	6	0	0
MCULE-3605396400	0	–1	364.5	–3.2	2	6.25	0	0
Maybridge3_002654	1	0	333.4	–0.3	0	5.5	0	0
Maybridge4_001571	1	1	388.2	–0.6	1	3.5	1	1
MCULE-2052162600	1	0	396.9	–1.1	0	3.75	1	1
MCULE-7340940770	0	–2	324.3	–1.9	1	6.25	0	0
MCULE-9673912218	0	–1	347.8	–2.7	1	6.5	0	0
MCULE-9823052966	1	1	349.5	–1.6	0	3.5	0	–1
MCULE-1671250996	0	–2	320.4	–2.8	1	6.5	0	0
Maybridge2_000711	0	–1	346.4	–2.1	0	6	0	0
Maybridge4_002924	1	0	372.4	–1.1	1	5.5	0	1
Maybridge1_002666	0	–2	244.3	–2.6	1	3.5	0	0
Maybridge1_008414	2	1	347.3	–1.5	2	1.5	1	1
MCULE-8839595892	2	2	379.8	0.1	0	2.3	1	1
MCULE-2164314832	1	0	285.7	–0.9	0	4	0	0
MCULE-9571013095	0	–1	298.3	–1.4	1.25	5	0	0
Maybridge3_003389	0	–1	337.4	–2.1	1	7	0	0
MCULE-8689473472	0	–1	382.3	–2.8	1	6.5	0	1
MCULE-9628232293	1	1	408.9	–1.1	0	3.5	1	1
MCULE-6342322238	1	0	343.4	–1.9	1	4.5	0	1
MCULE-8320211624	1	–1	350.4	–1.1	0.5	4	0	1

^aNumber of computed properties which fall outside the required range for 95% of known drug.

^bActivity in the central nervous system.

^cMolar weight.

^dThe predicted skin permeability.

^eNumber of hydrogen bonds donated by the molecule.

^fNumber of hydrogen bonds accepted by the molecule.

^gNumber of violations of Lipinski's 'rule of five'.

^hNumber of violations of Jorgensen's 'rule of three'.

molecule in the toxicity analysis did not present any alert, a fact that could be justified considering the low concentration in which it acts in the active site (Andrighetti, Cerone, Riguetti, Galvani, & Macoris, 2008; Itoh, 1982).

Analysis of the toxicological properties indicated that, of the 22 molecules, 10 show toxicity alerts characterized as 'plausible' or 'acceptable' and 12 did not present any type of alert. The description of the alert is related to the presence of constituent groups of the molecules, and thus, classify them as toxicophoric groups.

Phenol activity has been demonstrated in several skin sensitization assays, including the dermal sensitivity test in guinea pigs (Cronin & Basketter 1994) and the human maximization test (Opdyke, 1979). Phenol itself is corrosive, but is not a sensitizer (Basketter, Flyvholm, & Menne, 1999; Itoh, 1982). In simple phenols, it is thought that skin sensitization arises as a result of the formation of a phenolic radical which subsequently reacts with skin proteins, especially at the ortho positions of the phenol group (Barratt & Basketter, 1992), as observed in molecule MCULE-3605396400. Studies of QSAR have shown that, for other toxic pathways that also involve the formation of phenolic radicals, the activity of estrogens, such as estradiol, appears to be appropriately modelled, bringing the structure of a dialkyl-substituted phenol closer (Zhang, Gao, Hansch, & Selassie, 1998).

The hepatotoxicity alert is indicated by the presence of the thiazole group and its derivatives. These have been shown to cause elevation of hepatic enzymes, jaundice, cholestasis and steatosis in humans (Jalota & Freston, 1974; Picard, Rosmorduc, & Cabane, 1998; Skandrani et al., 2008), as observed in the warnings in molecules MCULE-2052162600 and MCULE-9823052966. The mechanism of

toxicity for this class is believed to involve epoxidation of the thiazole ring followed by ring cleavage leading to the formation of thioamide reactive metabolites. A good correlation between the hepatotoxicity of the 2-phenylthiazole derivatives and their proposed thioamide metabolites provides evidence of the proposed mechanism of toxicity (Mizutani & Suzuki, 1996).

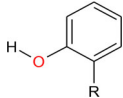
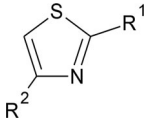
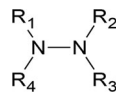
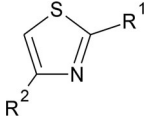
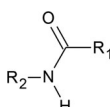
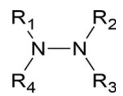
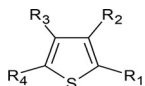
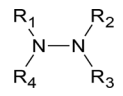
The presence of a skin-sensing structural alert within a molecule indicates that the molecule has the potential to cause skin sensitization. Thus, whether or not the molecule will be a skin sensitizer will also depend on its percutaneous absorption. Generally, small lipophilic molecules, like MCULE-9673912218 are more readily absorbed by the skin and therefore more prone to sensitization (Kayser & Schleder, 2001).

Considering the carcinogenic activity, nitro-aromatic compounds generally require metabolism for hydroxylamine aromatic intermediates (Holder, 1999; Takahashi et al., 1978; Miller, 1978), analogous to those involved in the carcinogenicity of aromatic amines, according to the Maybridge1_002666, MCULE-1671250996 and MCULE-8320211624 molecules.

Intestinal reduction by intestinal bacteria is an important metabolic pathway suspected of forming reactive intermediates from aromatic nitro compounds, while systemic nitroreductions can occur throughout the body. Pathways involving cytochrome P450 enzymes also contribute to the oxidative metabolism of many of these compounds. Alternatively, it has been proposed that aromatic nitro compounds can act through a mechanism involving the formation of reactive oxygen species and oxidative damage to DNA (Kovacic & Jacintho 2001).

There are distinct metabolic pathways that may vary in their relevance depending on the biological species as well as the electronic properties of the compounds (Schmitt,

Table 3. Predictions of the toxicological properties of selected molecules.

Molecule	ID	Prediction	Alert	Group
Pyriproxyfen	1	–	No alert	–
Maybridge3_005516	2	–	No alert	–
MCULE-3605396400	3	Skin sensitization	Plausible	
Maybridge3_002654	4	–	No alert	–
Maybridge4_001571	5	–	No alert	–
MCULE-2052162600	6	Hepatotoxicity	Plausible	
MCULE-7340940770	7	–	No alert	–
MCULE-9673912218	8	Skin sensitization	Plausible	
MCULE-9823052966	9	Hepatotoxicity	Plausible	
MCULE-1671250996	10	–	No alert	–
Maybridge2_000711	11	–	No alert	–
Maybridge4_002924	12	–	No alert	–
Maybridge1_002666	13	Carcinogenicity Hepatotoxicity	Plausible	
Maybridge1_008414	14	Carcinogenicity	Plausible	
MCULE-8839595892	15	–	No alert	–
MCULE-2164314832	16	–	No alert	–
MCULE-9571013095	17	–	No alert	–
Maybridge3_003389	18	Carcinogenicity Nephrotoxicity	Plausible	
MCULE-8689473472	19	Skin sensitization	Plausible	
MCULE-9628232293	20	–	No alert	–
MCULE-634232238	21	Hepatotoxicity	Plausible	
MCULE-8320211624	22	Carcinogenicity Hepatotoxicity Skin sensitization Teratogenicity	Plausible	

Altenburger, Jastorff, & Schuurmann, 2000). The proposed mechanisms of toxicity involve the initial reduction of the nitro group to form the nitro anion radical. Gradual

reductions under hypoxic conditions lead to nitrous and hydroxylamine metabolites, which have increased electrophilia to interact with electron-rich sites of macromolecules.

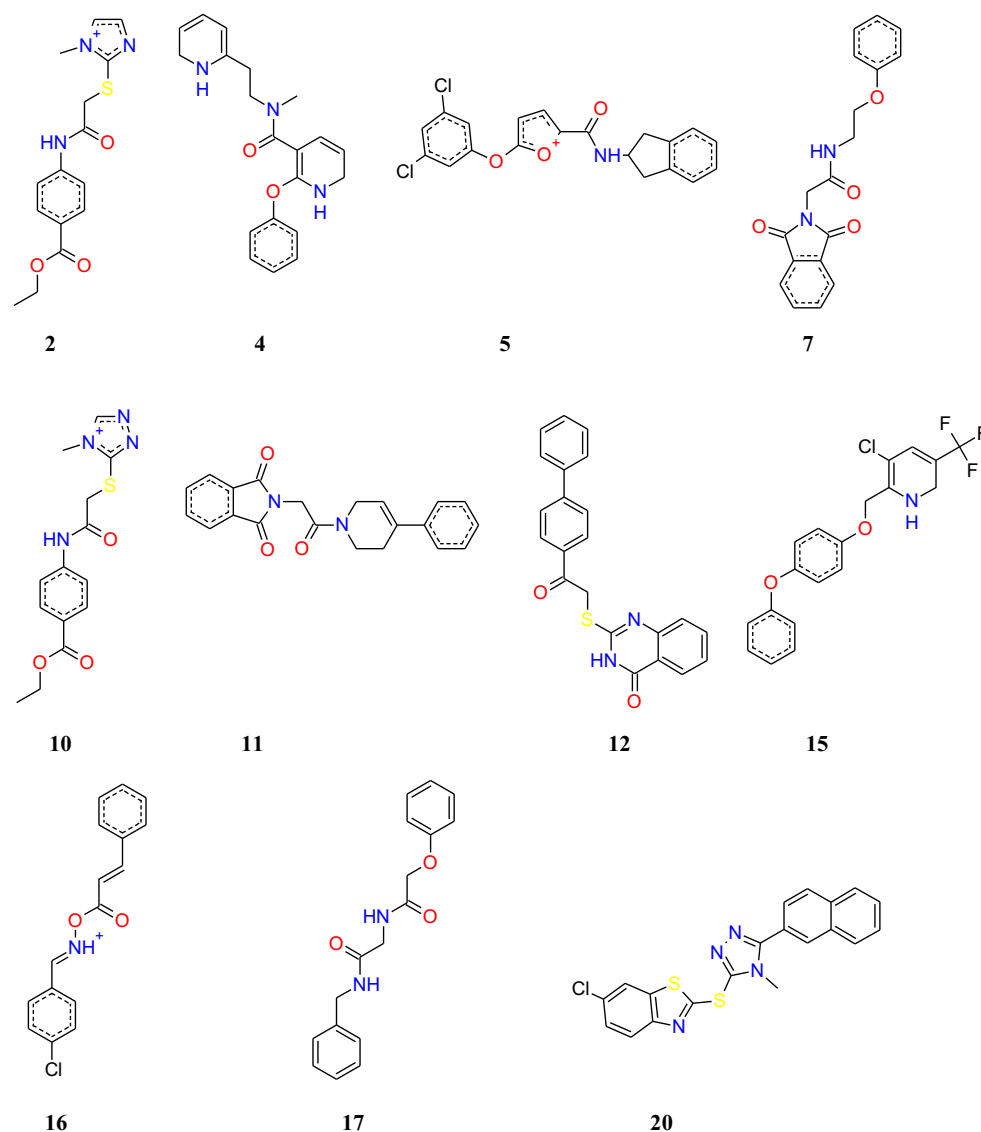


Figure 2. 2D structures of selected molecules containing good pharmacokinetic and toxicological profiles.

Table 4. Biological activity prediction of the compounds selected by virtual screening approaches.

Molecules	Pa ^a	Pi ^b	Biological activity
Pyriproxyfen	0.586	0.003	Insecticide
GNT	0.376	0.154	Acetylcholine neuromuscular blocking agent
I40	0.025	0.005	Acetylcholine transporter inhibitor
JHIII	0.336	0.011	Insecticide
Maybridge3_005516	0.211	0.197	Acetyl esterase inhibitor
Maybridge3_002654	–	–	–
Maybridge4_001571	–	–	–
MCULE-7340940770	0.437	0.043	Acetyl esterase inhibitor
MCULE-1671250996	0.211	0.197	Acetyl esterase inhibitor
Maybridge2_000711	0.618	0.019	Acetyl esterase inhibitor
Maybridge4_002924	0.267	0.124	Acetyl esterase inhibitor
MCULE-8839595892	0.349	0.010	Insecticide
MCULE-2164314832	0.209	0.034	Insecticide
MCULE-9571013095	0.361	0.164	Acetylcholine neuromuscular blocking agent
MCULE-9628232293	–	–	–

^aPa = probability to be active.

^bPi = probability to be inactive.

The aromatic amines according to the group present in the molecule Maybridge1_008414 and MCULE-1671250996

may act as genotoxic chemical carcinogens after metabolic activation (Williams & Weisburger, 1993). The mechanism of action is generally considered to proceed through N-hydroxylation with subsequent O-esterification to form, in most cases, O-acetylated or O-sulphated derivatives (Andersen, Enomoto, Miller, & Miller, 1964).

The nephrotoxicity of the non-steroidal anti-inflammatory drugs (NSAIDs) of arylacetic acid or 2-arylpropionic acid and its fulvenil derivatives, as per the alert in molecule MCULE-1671250996. Non-steroidal anti-inflammatory compounds lead to several well-established and mechanistically distinct forms of nephrotoxicity in man and other mammals. Exemplary compounds include fenoprofen (Biscarini, 2000; Porile, Bakris, & Garella, 1990), diclofenac (Inoue et al., 2008) and tolmetin (Pascoe, Gordon, & Temple-Camp, 1986), which were all associated with a high incidence of idiosyncratic acute renal failure dose independent.

Alert of the molecule MCULE-6342322238 describes that the hepatotoxicity of these compounds results from the metabolic activation of the thiophene ring, mainly mediated by cytochrome P450. The initial activation of a thiophene

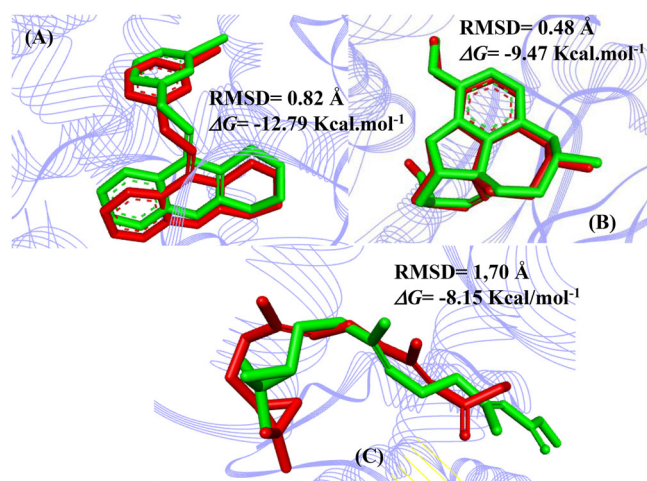


Figure 3. Superpositions of the crystallographic poses (in green) with the docked ones (in red) of the compounds (A) I40, (B) GNT and (C) JHIII, and respective RMSD and ΔG values.

epoxide was postulated to lead to the formation of mercapturate intermediates (O'donnell, Dalvie, Kalgutkar, & Obach, 2003; Treiber et al., 1997) and also to the cleavage of the ring generating an alpha, beta-unsaturated aldehyde (Dalvie, Kalgutkar, Khojasteh-Bakht, Obach, & O'Donnell, 2002).

Hydrazines are used as synthetic intermediates in the chemical industry and as therapeutic agents for the treatment of tuberculosis, depression and cancer. The teratogenicity of hydrazines can be due to two distinct mechanisms: (i) direct binding (e.g. 1,1-dimethylhydrazine and hydrazine) by its free amino group to biomolecules such as vitamin B6 and (ii) generation of reactive species of radicals free and electrophilic entities (carbon ions, acylation species and diazonium) by metabolic activation (Kalgutkar et al., 2005).

Biological activity prediction

Using virtual screening with the ROCS and EON software, respectively, we selected the top-ranked molecules, which were subsequently subjected to pharmacokinetic predictions, resulting in 21 molecules with a good pharmacokinetic profile, and only 12 showed no toxicity alert. Selected molecules showing good pharmacokinetic and toxicological profiles can be visualized in Figure 2.

Prediction of biological activity using the Web server PASS [35] resulted in the data shown in Table 4. The reference/template compounds here used (pyriproxyfen, I40, GNT and JHIII) showed insecticidal activity, corroborating results found in the literature (Harburguer et al., 2009; Harwood et al., 2016; Olmstead & Leblanc, 2003; Paul, Harrington, & Scott, 2006; Sullivan & Goh, 2008).

The molecules Maybridge3_005516, MCULE-7340940770, MCULE-1671250996, Maybridge2_000711, Maybridge4_002924, MCULE-8839595892, MCULE-2164314832 and MCULE-9571013095 have shown satisfactory predictions for acetylcholine activity, acetylcholine antagonist and acetyl esterase inhibitor and acetylcholine neuromuscular blocking agent, all with P_a ranging 0.209–0.586, being similar to other known bioactive compounds, when $P_a > P_i$.

Molecular docking study

Validation of the molecular docking protocols here used was performed using the crystallographic structures of the reference/template compounds, in which the docking poses should be similar to the respective crystallographic ones (from the PDB IDs 1QON and 4EY6, for AChE, and PDB ID 5V13 for the juvenile hormone).

Recovering the pose of each AChE inhibitor (I40 and GNT) as well as the juvenile hormone (JHIII), it was possible to perform the validation of the molecular docking protocols, calculating mean square deviation values (RMSD) of 0.82, 0.48 and 1.70 Å, respectively. According to Gowtham, Jayakanthan, and Sundar (2008) and Hevener et al. (2009), the predicted binding mode using docking indicates that when the mean square distance (RMSD) is <2.0 Å with respect to the crystallographic pose of a respective inhibitor, validation is considered satisfactory. The best results can be seen in Figure 3.

The resultant docking pose enabled the inhibitor to also bind to the amino acid residues of the active site of I40 (PDB ID 1QON) around the α -helix located between the amino acid residues Thr369–Asp375 and comprised in the β -sheet located between the residues of amino acids Ile82–Trp83. Regarding the inhibitor, it is possible to observe hydrophobic interactions with the vast majority of residues in Tyr71, Trp83, Tyr370, Phe371, Tyr374 and His380, which results are in agreement with the studies of Harel et al. (2000).

The GNT compound (PDB ID 4EY6) showed interactions between the α -helix residues Ser336–Leu339 and Ser337–Leu339 and between the β -sheet residues Met86–Trp87, Gly121–Tyr124 and Glu202–Ser203. Thus, it becomes possible to classify the interactions of hydrogens with Glu202 and Ser203 and van der Waals with Tyr124 and His447. There are hydrophobic interactions with residues Trp86, Gly121, Tyr337 and Phe338, which are in agreement with the literature (Kim et al., 2017).

The interaction site of JHIII (PDB ID 5V13) showed interactions between the Leu33–Leu37, Ile44–Val51, Tyr59–Glu71 and Cys122–His136 amino acid residues at the α -helix and interactions between the Leu72–Arg73 residues at the β -sheet. The interactions were classified as the hydrophobic type for all the residues (Kim et al., 2017).

The potential inhibitors were evaluated according to the binding mode with the acetylcholinesterase (insect/human) and juvenile hormone receptors and of the eleven molecules submitted to the docking protocols, only five had interactions similar to the observed with the controls/reference molecules used, and of these five, two are identical binding modes in all the proteins here used.

The interactions were quantified in terms of binding affinity regarding the controls (I40, GNT and JHIII) for acetylcholinesterase from different organisms (*Drosophila melanogaster* and *Homo sapiens*) as well as for the juvenile mosquito hormone (*Aedes aegypti* organism) and the new potential inhibitors. The affinity values of the new potential inhibitors of the acetylcholinesterase (from *Drosophila melanogaster*) can be seen in Figure 4.

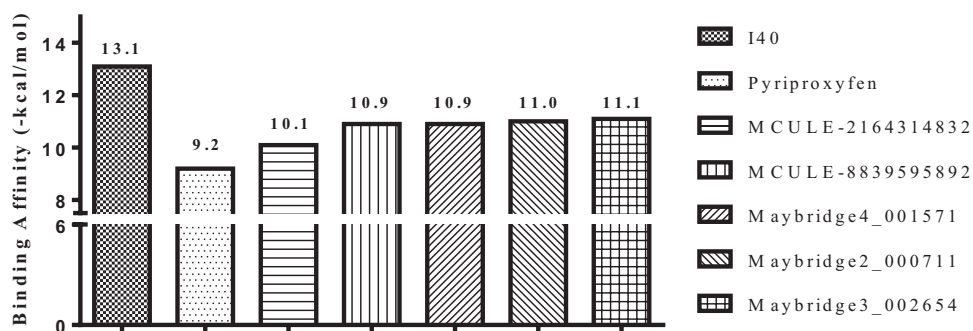


Figure 4. Results of binding affinity of the compounds with insect acetylcholinesterase (*Drosophila melanogaster* organism) - Protein Data Bank (PDB) ID 1QON.

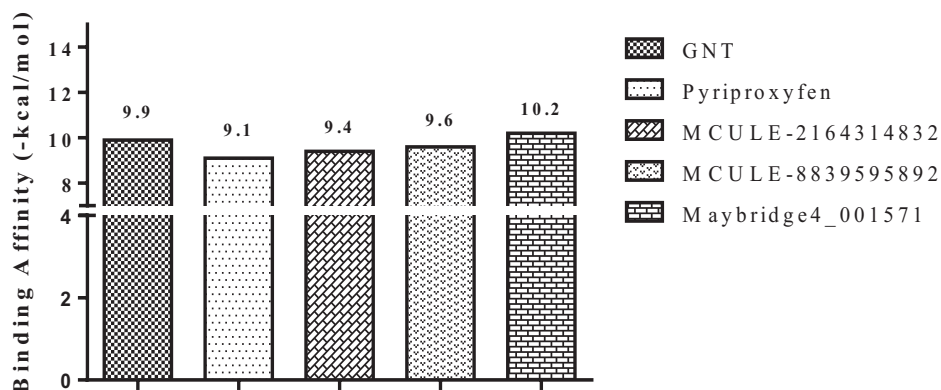


Figure 5. Results of binding affinity of the compounds with human acetylcholinesterase (*hAChE*) - PDB ID 4EY6.

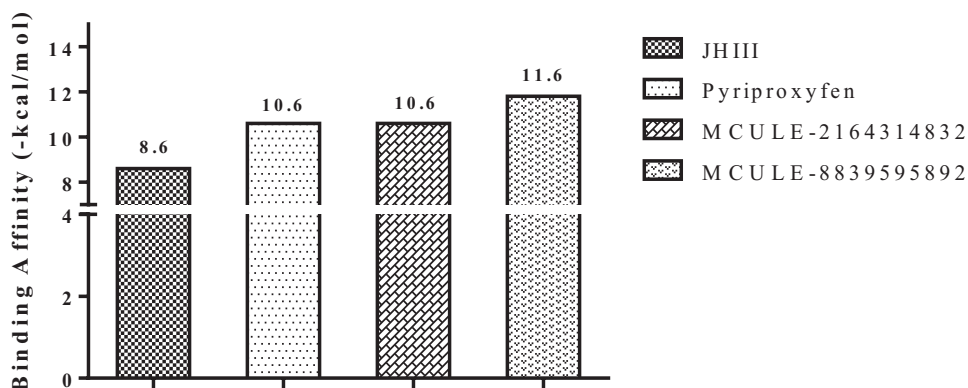


Figure 6. Results of binding affinity of the compounds with the juvenile hormone receptor (PDB ID 5V13).

Inhibitors complexed with the acetylcholinesterase enzyme had higher values than the control pyriproxyfen (*template*) and smaller than the I40 control, whereas the inhibitors Maybridge2_000711 and Maybridge3_002654 show values of affinity of -11.0 and -11.1 kcal/mol, respectively. The molecules are shown to be promising for insecticidal activity, since they have similar interactions to the observed for the controls here used in the docking studies. I40 exhibited a difference of ± 3.9 kcal/mol compared to pyriproxyfen. However, intense interaction was observed compared to other potential inhibitors, since there was a difference between the affinity values that varied among ± 3.0 (MCULE-2164314832); ± 2.2 (MCULE-8839595892); ± 2.2 (Maybridge4_001571); ± 2.1 (Maybridge2_000711) and ± 2.0 (Maybridge3_002654) kcal/mol.

In the human acetylcholinesterase, the new inhibitors had higher binding affinity as well as free energy values than the

controls used in the molecular docking studies here performed. Thus, the results suggest insecticidal activity for the inhibitors, since the molecules present a significant similarity of interactions with active site of the enzyme. It is worth of note the Maybridge4_001571, MCULE-8839595892 and MCULE-2164314832 molecules, which showed binding affinity values of -10.2 , -9.6 and -9.4 kcal/mol, respectively, according to Figure 5.

Molecules complexed to the acetylcholinesterase enzyme had higher binding affinity values compared to the control pyriproxyfen, and of these only Maybridge4_001571 was higher than GNT. GNT showed a difference of ± 0.8 kcal/mol compared to pyriproxyfen, and compared to the two controls, the molecule Maybridge4_001571 shows a higher binding affinity, with difference of ± 0.3 kcal/mol (in relation to GNT) and ± 1.1 kcal/mol (in relation to pyriproxyfen), which

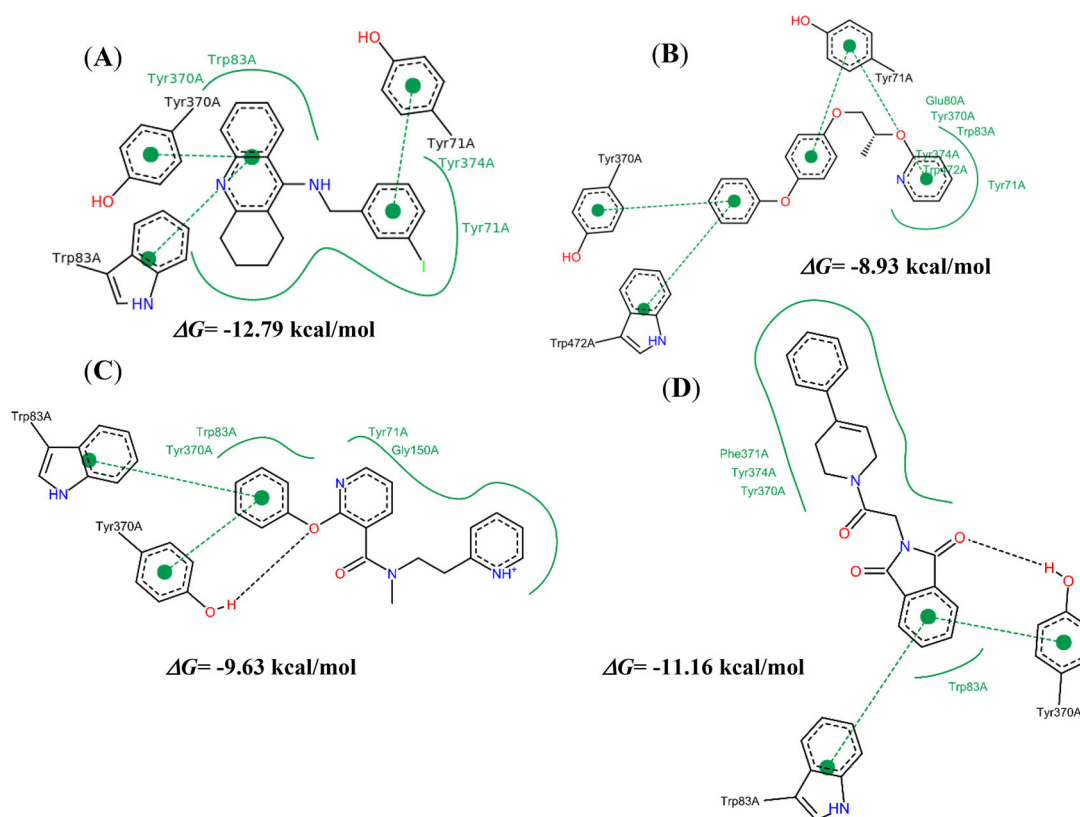


Figure 7. Interactions of the I40 (A), pyriproxyfen (B) and potential Maybridge3_002654 (C) and Maybridge2_000711 (D) inhibitors with the insect acetylcholinesterase active site (PDB ID 1QON)*. *Black dashed lines indicate hydrogen bonds, salt bridges and metal interactions. Solid green lines show hydrophobic interactions and dashed greens show π - π and π -cations interactions.

can be inferred that it has high affinity to the active site of the human acetylcholinesterase.

Regarding the juvenile hormone receptor, a high binding affinity value of the tested ligands was observed compared to the JHIII and pyriproxyfen controls here used in the molecular docking studies. The affinity values of the controls and ligands can be visualized in Figure 6.

The potential inhibitors MCULE-2164314832 and MCULE-8839595892 were shown to have higher binding affinity than the controls here used in the docking studies, with -10.6 kcal/mol and -11.6 kcal/mol, respectively. The difference between the MCULE-8839595892 inhibitor and the pyriproxyfen control was ± 1.0 kcal/mol, indicating that such inhibitor is considered to have a dual action mechanism because it interacts with other insect/human acetylcholinesterase as a potential insecticidal agent or retarding the growth process or cause poor morphological formation of the *Aedes aegypti*.

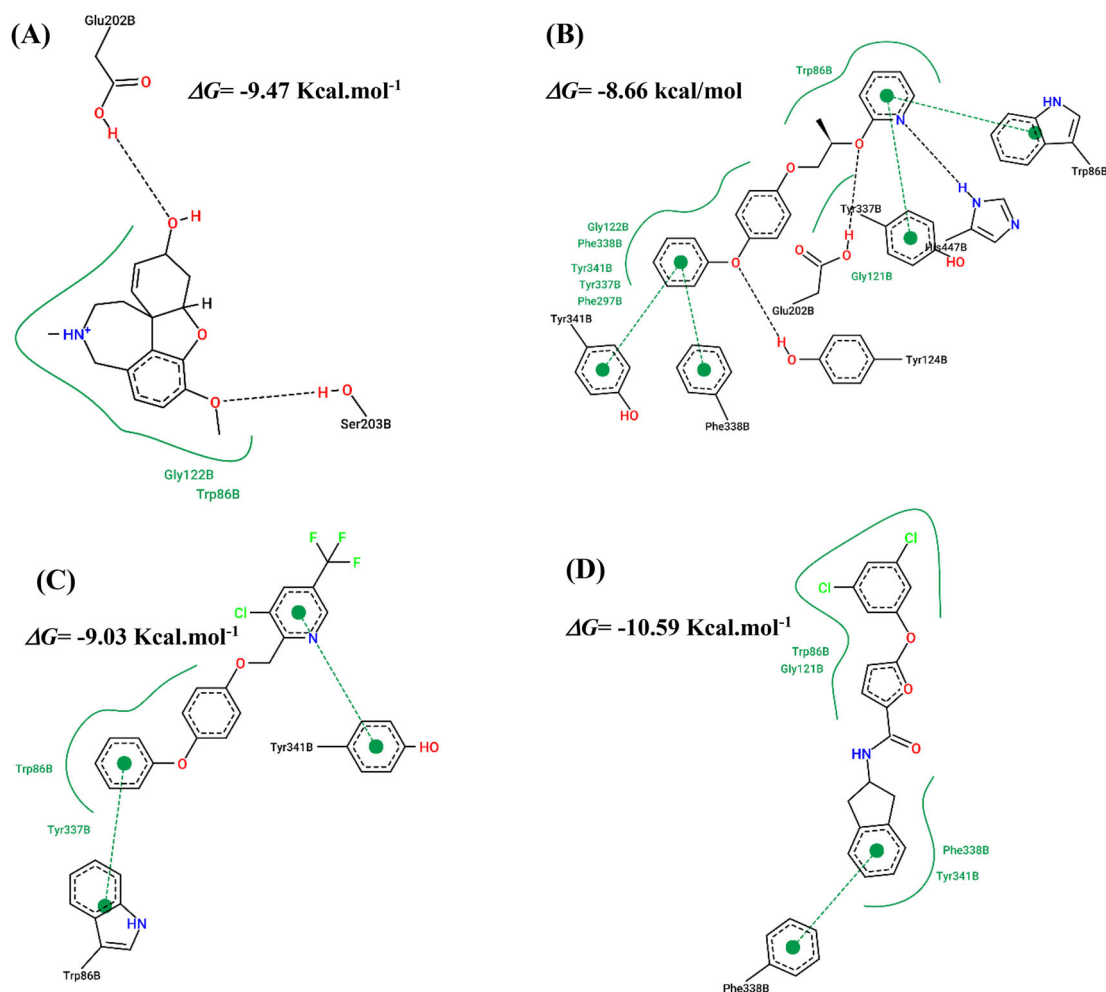
The interactions observed for the I40 and pyriproxyfen controls in the docking studies were also similar regarding the Maybridge3_002654 and Maybridge2_000711 molecules relative to the acetylcholinesterase active site, located around the α -helix between the amino acid residues Tyr370–Tyr374 and the β -sheet (at the Trp83 residue), according to Figure 7.

The main function of the acetylcholinesterase enzyme is to remove the acetylcholine accumulated in the synaptic cleft caused by the processes of propagation of the nervous impulse, so the acetylcholine when interacting with the enzyme ends up inactivating it for the cycle to continue

(Pizova et al., 2017). The insecticidal activity is described as acting of a substance directly in the CNS, which causes some type of alterations of the metabolic functions essential for maintenance of organs to maintain the daily activities, in this way, causing the death by collapse of the nervous system. Chemically, the acetylcholinesterase enzyme is inactivated with these highly reactive molecules, causing a greater accumulation of acetylcholine in the synaptic cleft, and because of this increased concentration, the nerve functions enter into dysfunction and eventually organism death.

In the molecular docking study here performed, the interactions of our potential inhibitors with the amino acid residues Trp71, Trp83, Tyr370, Phe371 and His480 of acetylcholinesterase are similar to those reported in the literature (Fournier, Mutero, Pralavorio, & Bride, 1993; Gnagey, Forte, & Rosenberry, 1987). The best inhibitors evaluated regarding binding affinity were 19582 and 45353, in which the interactions were similar to those observed for the controls I40 and pyriproxyfen, with the residues Tyr71, Trp83, Tyr370 and Tyr374, contributing to the increase of the binding affinity. The less common interactions between the inhibitors were Glu80, Gly150 and Phe371, where such contributions could inactivate the AChE of the insect.

Regarding the molecule Maybridge2_000711, with free energy of -9.63 kcal/mol, it shows hydrogen bond with the residue Tyr370, as well as an π - π interaction with Trp83, similarly to the observed for I40. The molecule Maybridge3_002654, with higher potential for insecticidal activity, has higher free energy than the control pyriproxyfen



* Black dashed lines indicate hydrogen bonds, salt bridges, and metal interactions. Solid green lines show hydrophobic interactions and dashed greens show π - π and π -cations interactions.

Figure 8. Interactions of GNT (A), Pyriproxyfen (B) and potential inhibitors MCULE-8839595892 (C) and Maybridge4_001571 (D) with the acetylcholinesterase active site (PDB ID 4EY6) *. *Black dashed lines indicate hydrogen bonds, salt bridges and metal interactions. Solid green lines show hydrophobic interactions and dashed greens show π - π and π -cations interactions.

(−8.93 kcal/mol), and it similarly makes π - π interaction with Tyr370. However, the interactions are more intense in the inhibitor, thus favoured by a reduction of the interaction distance. The conformation of the inhibitors in the active site is influenced by the distances of the interactions with the amino acid residues.

Regarding the GNT and pyriproxyfen controls here used in the docking studies, similar interactions were detected for the molecules MCULE-8839595892 and Maybridge4_001571 in relation to the acetylcholinesterase active site, located around the α -helix (between the amino acid residues Ser203, Tyr337 and Phe338) and in the β -sheet (between residues Trp86, Gly121 and His447), as shown in Figure 8.

According to Meriç (2017), in the AChE active site the catalytic triad (Ser203, Glu334 and His447) is found in the lower portion of the active site, surrounded by three important characteristics for the catalytic activity: the acyl bag (residues of Phe295, Phe297 and Phe338), the oxy-anion channel (main residue nitrogen Gly121, Gly122 and Ala204) and the choline binding site (Trp86 and Tyr337). The most significant contributions of the interactions, according to the present

docking study, are observed for the molecule Maybridge4_001571, in which the contribution of the catalytic triad (represented by His447) and the binding of the inhibitor to the Trp86 choline site is remarkable. Other uncommon interactions have also been observed with residues Tyr124, Tyr341 and Glu202, and such interactions eventually stabilize the ligand at the active site of the enzyme. The increase in the binding affinity, in turn, inactivates the enzyme acetylcholinesterase by competition with GNT by the active site.

In the juvenile hormone receptor complexed with JHII or the control pyriproxyfen, similar interactions were observed for the molecules MCULE-2164314832 and MCULE-8839595892 present among the amino acid residues located around the α -helix (between the amino acid residues Tyr33, Leu37, Val51, Val68 and Tyr129) and the β -sheet (between the amino acid residues Trp53 and Phe144), as shown in Figure 9.

The molecule MCULE-2164314832, with free energy of −10.41 kcal/mol, shows hydrophobic type interactions with residues Tyr33, Val51, Val68 and Tyr129 as well as π - π

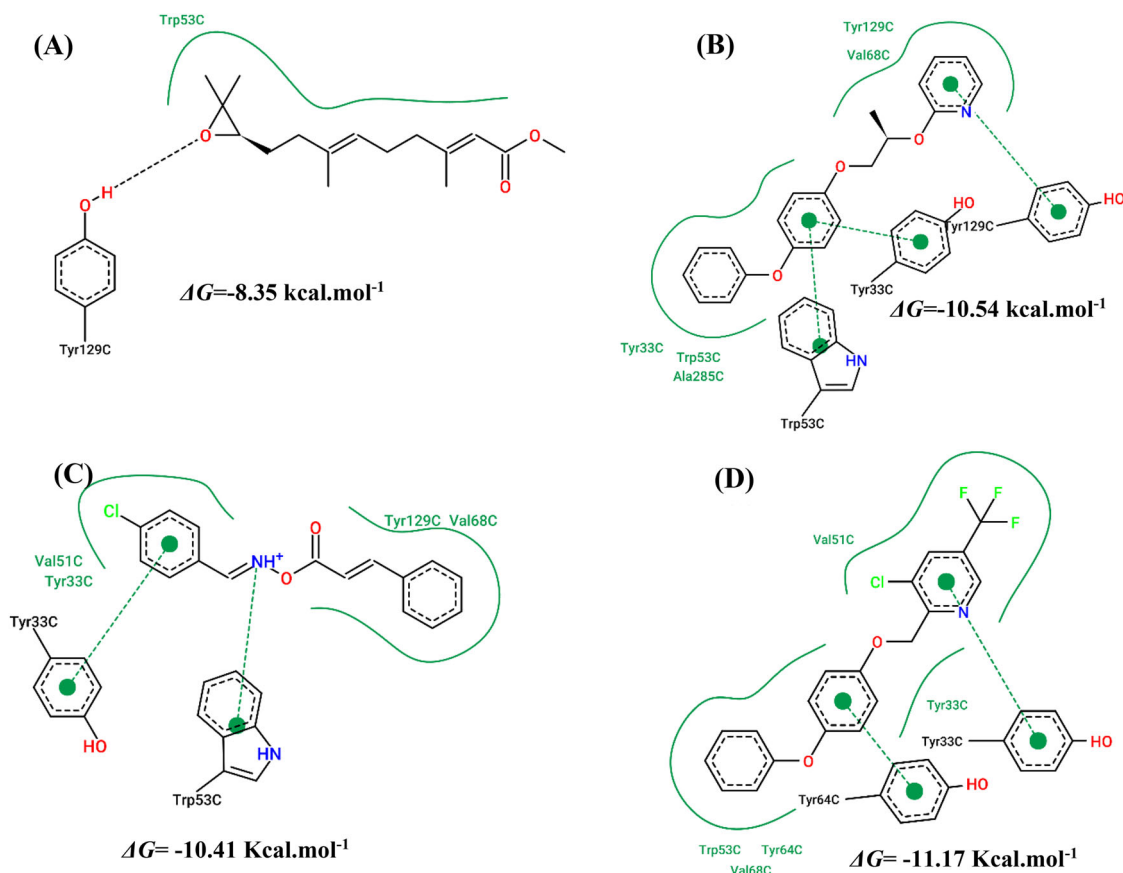


Figure 9. Interactions of JHIII (A), Pyriproxyfen (B) and potential MCULE-2164314832 (C) and MCULE-8839595892 (D) inhibitors with the hormone receptor site*. *Black dashed lines indicate hydrogen bonds, salt bridges and metal interactions. Solid green lines show hydrophobic interactions and dashed greens show π - π and π -cations interactions.

Table 5. Oral toxicity prediction results for input compounds.

Molecule	Predicted LD ₅₀ (mg/kg)	Predicted toxicity class ^a
Pyriproxyfen (control)	2000	IV
I40	200	III
GNT	19	II
JHIII	5000	IV
Maybridge3_002654	1000	IV
Maybridge4_001571	1860	IV
Maybridge2_000711	1190	IV
MCULE-8839595892	518	IV
MCULE-2164314832	921	IV

^aClass I: fatal if swallowed (LD50 < 5); Class II: fatal if swallowed (5 < LD50 < 50); Class III: toxic if swallowed (50 < LD50 < 300); Class IV: harmful if swallowed (300 < LD50 < 2000); Class V: may be harmful if swallowed (2000 < LD50 < 5000); Class VI: non-toxic (LD50 > 5000).

interactions with Trp33 and Trp53. The molecule with the greatest potential to inhibit the acetylcholinesterase enzyme is MCULE-8839595892, because it makes similar significant interactions and it has free energy of -11.17 kcal/mol, compared to the controls here used. There are less common interactions for the Val34 and Tyr64 residues, which contribute to greater stability of the molecule to the receptor.

In the juvenile hormone protein complex, the JHIII linker is present in the N-terminal domain binding pocket, where the crystallographic conformation is identical at the three chains/subunits of the protein. In the JHIII, the presence of an epoxy group is observed located at the centre of the domain and a methyl ester is oriented toward the surface.

Table 6. Molecules selected in the *in silico* study.

N°	Molecule	ID
4		Maybridge3_002654 MolPort-001-808-490
5		Maybridge4_001571 MolPort-001-808-749
11		Maybridge2_000711
15		MolPort-002-899-880 MCULE-8839595892
16		MCULE-2164314832

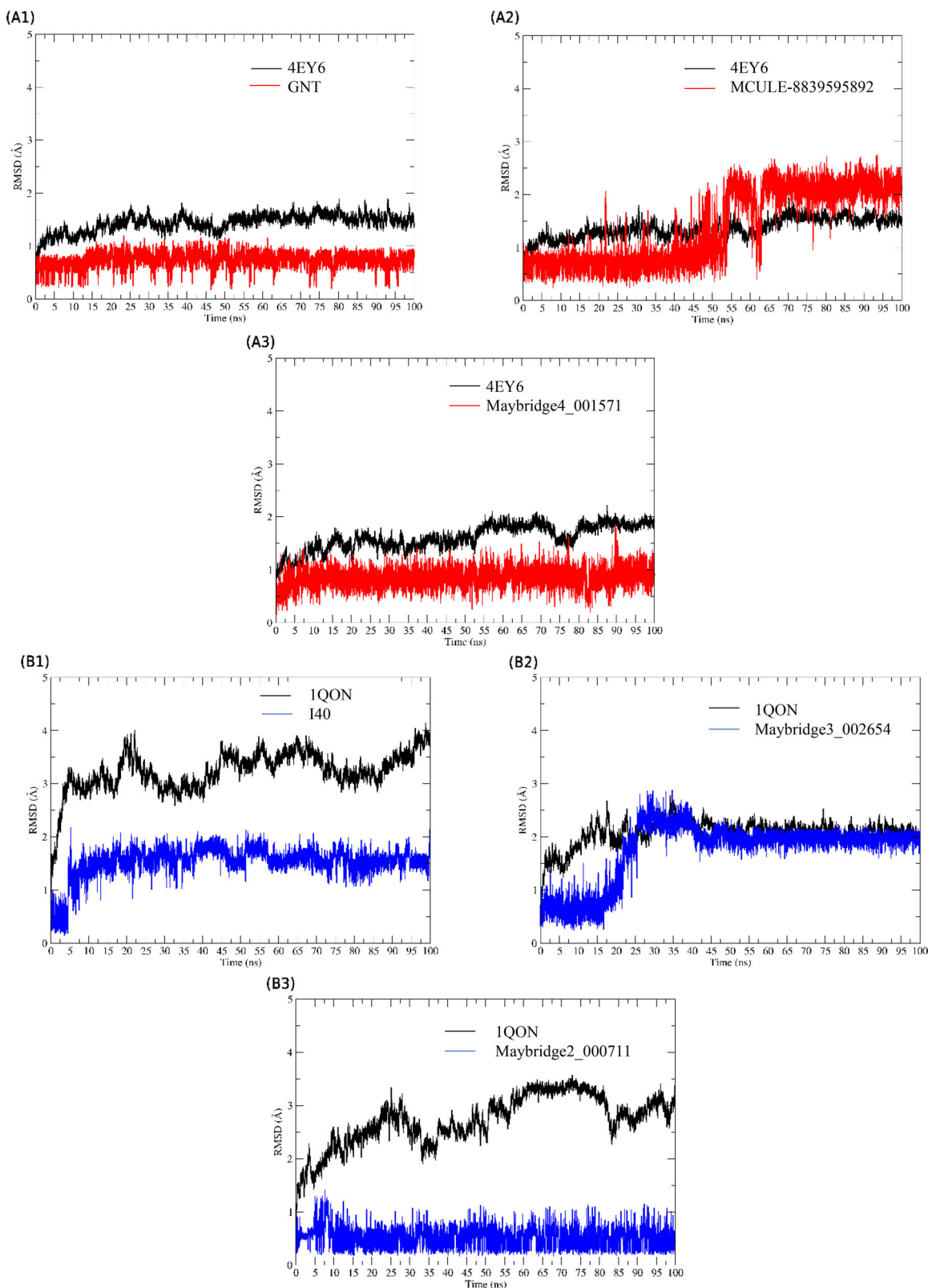


Figure 10. RMSD plots of the established systems with the enzymes (A1, A2 and A3) AChE human, (B1, B2 and B3) AChE of *Drosophila melanogaster* and (C1, C2 and C3) juvenile Hormone (*Aedes aegypti*).

The epoxy group makes hydrogen bonds with the phenolic hydroxyl of Tyr129 and the remainder of the isoprenoid chain is surrounded by hydrophobic side chains, including those of Phe144, Tyr64, Trp53, Val65, Val68, Leu72, Leu74, Val51 and Tyr33 (Drwal et al., 2014).

Toxicity risk assessment

Lethal dose 50 (LD₅₀) values are reported in (mg/kg) according to World Health Organization (WHO) classifications, which identify five groups based on oral LD₅₀ (Rat Categories) rat

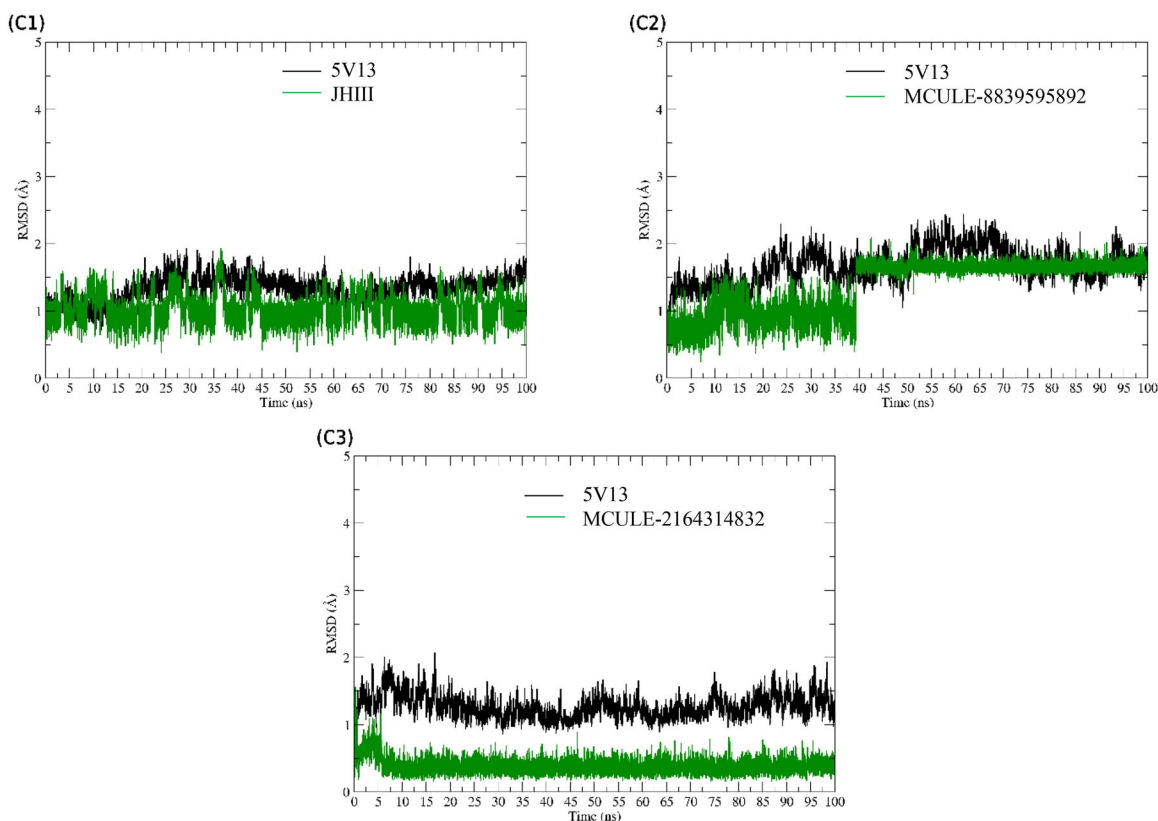


Figure 10. (Continued).

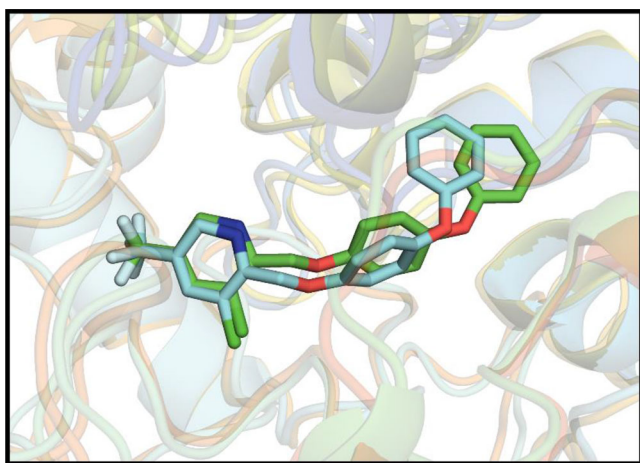


Figure 11. Superposition of the inhibitor structure in different simulation times: simulation times from 0 to 50 ns (green) and 51 to 100 ns (blue).

data (Banerjee, Dehnbostel, & Preissner, 2018; Banerjee, Eckert, Schrey, & Preissner, 2018; Coscollà, Vicent, Martí, & Pastor, 2008; Drwal et al., 2014; Yang et al., 2014; WHO, 2009).

Severity of the effects depends on the classification of the pesticides and the dose of exposure as well. The molecules used in this step do not violate the Lipinski's Rule of Five, as can be seen in Table 1. Predicted LD50 values of the compounds here investigated are described in Table 5.

Oral toxicity values defined for the molecules were 2000 (mg/kg) for pyriproxyfen (control), 1000 (mg/kg) for Maybridge3_002654, 1860 (mg/kg) for Maybridge4_001571, 1190 (mg/kg) for Maybridge2_000711, 518 (mg/kg) for MCULE-8839595892 and 921 (mg/kg) for MCULE-2164314832,

respectively. Molecules are classified as belonging to class IV ($300 < LD50 \leq 2000$), harmful if swallowed.

Structure–activity relationship of the promising molecule

At the end of the virtual screening stages, five molecules presented better profile for the insecticidal potential, being (4) classified as alkaloid, (5) carboxamide with a furan group, (11) indole group, (15) pyridine and (16) group according to Table 6.

The molecule 4 has in its structure a pyridine, a carboxamide as well as a phenoxy group, and 15 has a pyridine group which act on the chemical and physical properties. Such groups classify the structure as belonging to classes of secondary metabolite of the alkaloids. The pyridine group may act as competitive modulators of nicotinic acetylcholine receptors. The wide spectrum of biological activities is reported to alkaloids and may be related to their structural variety, such as the anticholinergic, sympathomimetic, antiviral, insecticidal, Alzheimer's and many others (Lipinski et al., 2001; Silva et al., 2019). Vale and Lotti (2015) data show that more than 10,000 alkaloids have been described and constitute one of the most diverse and prominent groups of natural products of pharmacological and toxicological importance.

Crude extracts obtained from plants containing bioactive alkaloids, insecticides play an important role in insect reduction in agriculture and public health. In molecule 5, the furan and the carboxamide group act as inhibitors of succinate dehydrogenase II complex. In molecule 11, the indole group acts as a modulator of acetylcholinesterase and, in molecule 16, the imino group shows reactivity relative to $-NH^+$.

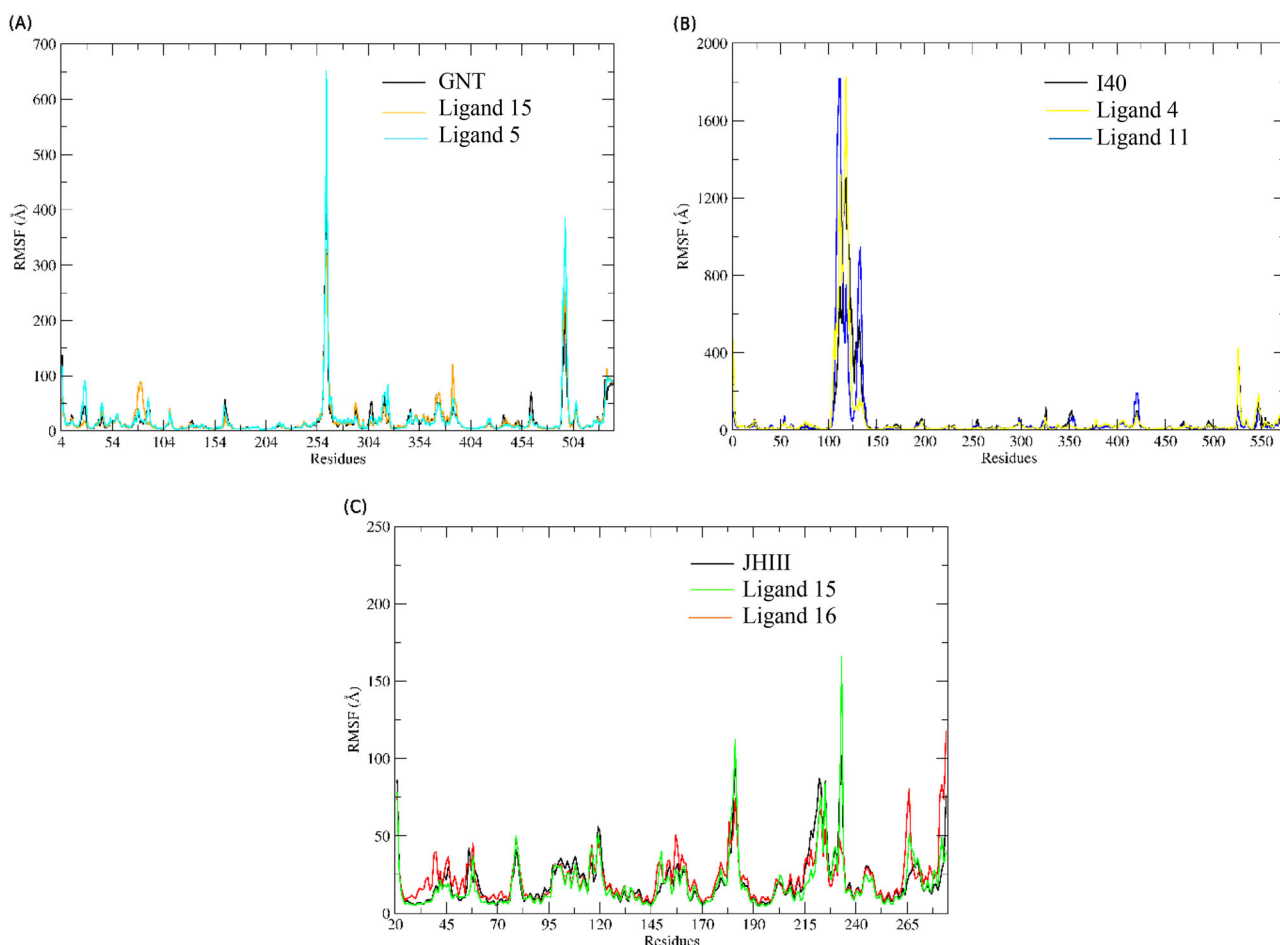


Figure 12. RMSF plot of the backbone of the proteins that established complex with the compounds used as control and with the inhibitors obtained by virtual screening. In black, the RMSF of the compounds used as control was represented, in order to plot the RMSF of the proposed inhibitors, several colours were used. (A) Plot of human AChE, (B) AChE of *Drosophila melanogaster* and (C) juvenile hormone *Aedes aegypti*.

Simulations of molecular dynamics

The structures **4**, **5**, **11**, **15** and **16** in the previous step were the ones that presented the best *in silico* results and followed to the molecular dynamics (MD) simulations with the aim of providing information about the microscopic behaviour along the time, observing each individual atom that composes the system. The molecules were treated as a collection of atoms described by Newtonian forces, where the particles are held together by harmonic or elastic forces. Structural analyses of the acetylcholinesterase systems (PDB IDs 1QON and 4EY6) and juvenile hormone (PDB ID 5V13) allowed us to observe molecular interactions at the binding site and the free energy of the components as well.

Structural analysis of the systems

To quantify the differences that occur along the time in the backbone structure of the proteins as well as the ligands, we plot the root mean square deviation (RMSD) curves. The backbone RMSD plot utilized the $C\alpha$ atoms of the amino acids. The *RMSD vs time* plots can be seen in Figure 10.

In all the figures the backbone of the enzymes was plotted in black colour, while the colour to represent the RMSD of the ligands was variable.

The RMSD values of the complexes formed by human AChE with the GNT control (A1) and the proposed inhibitors MCULE-8839595892 (A2) and Maybridge4_001571 (A3) are shown in A1, A2 and A3. In B1, B2 and B3, the RMSD values of the established systems with the enzyme AChE of *Drosophila melanogaster* complexed with the I40 (B1) control as well as the proposed inhibitors Maybridge3_002654 (B2) and Maybridge2_000711 (B3) are shown. The RMSD plot of inhibitors of the *Aedes aegypti* juvenile hormone enzyme can be visualized in C1 (control JHIII), MCULE-8839595892 (C2) and MCULE-2164314832 (C3).

Along the simulations, the reference ligands I40, GNT and JHIII remained stabilized at the AChE binding site of *D. melanogaster*, human AChE and the *Aedes aegypti* juvenile hormone protein, respectively.

The molecule Maybridge3_002654, which interacts with the AChE of *D. melanogaster* reached stability at ~ 45 ns and remained stable until the end of the MD simulation. The molecule Maybridge2_000711 achieved equilibrium more rapidly, from 10 ns, and it showed a tendency to remain stable at the protein binding site.

Novel compounds having activity against human AChE also showed good molecular stability when interacting with the pharmacological target. The molecule MCULE-8839595892 was stable at ~ 65 ns. The molecule Maybridge4_001571 showed great stability in its RMSD plot from ~ 10 ns.

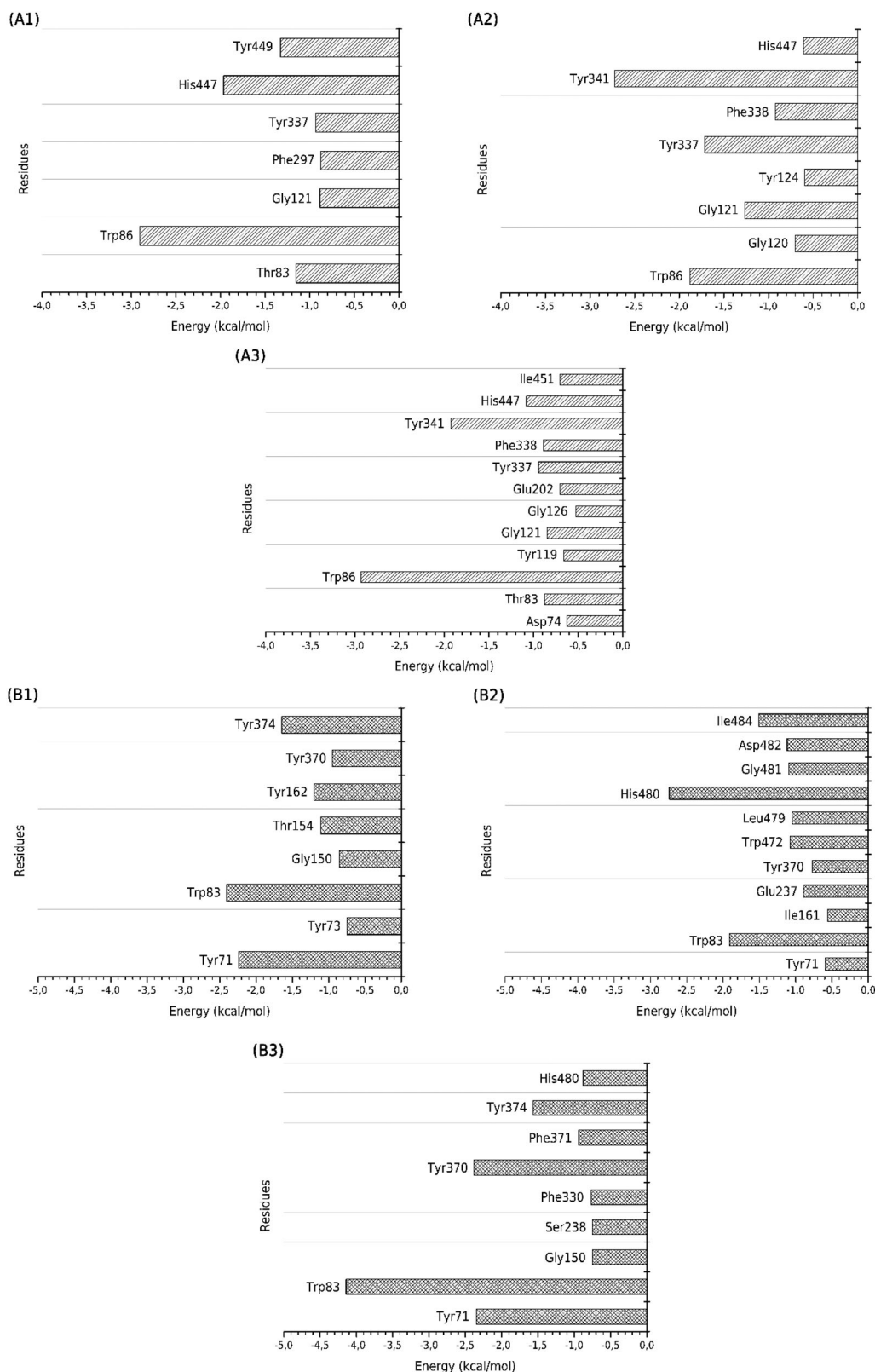


Figure 13. Per-residue free energy decomposition. The group of images A1, A2 and A3 correspond to the energy interaction values of the active site residues of human AChE that interacted with the GNT control compound and the ligands MCULE-8839595892 and Maybridge4_001571, respectively. The B1, B2 and B3 images represent residues from the catalytic cavity of *Drosophila melanogaster* AChE that interacted with the control molecule I40 and with the compounds Maybridge3_002654 and Maybridge2_000711, respectively. Energy juvenile hormone values protein binding site residues are displayed at C1, C2 and C3, representing the systems established with the control compound JHIII and with the proposed ligands MCULE-8839595892 and MCULE-2164314832, respectively.

MCULE-8839595892 (Figure 10.A2) at ~50 ns has undergone conformational changes, as can be seen in the variation of its RMSD graph.

This variation was quantified from the mean RMSD values calculated from 0 to 50 ns and from 51 to 100 ns. These periods were chosen because in these time ranges the largest

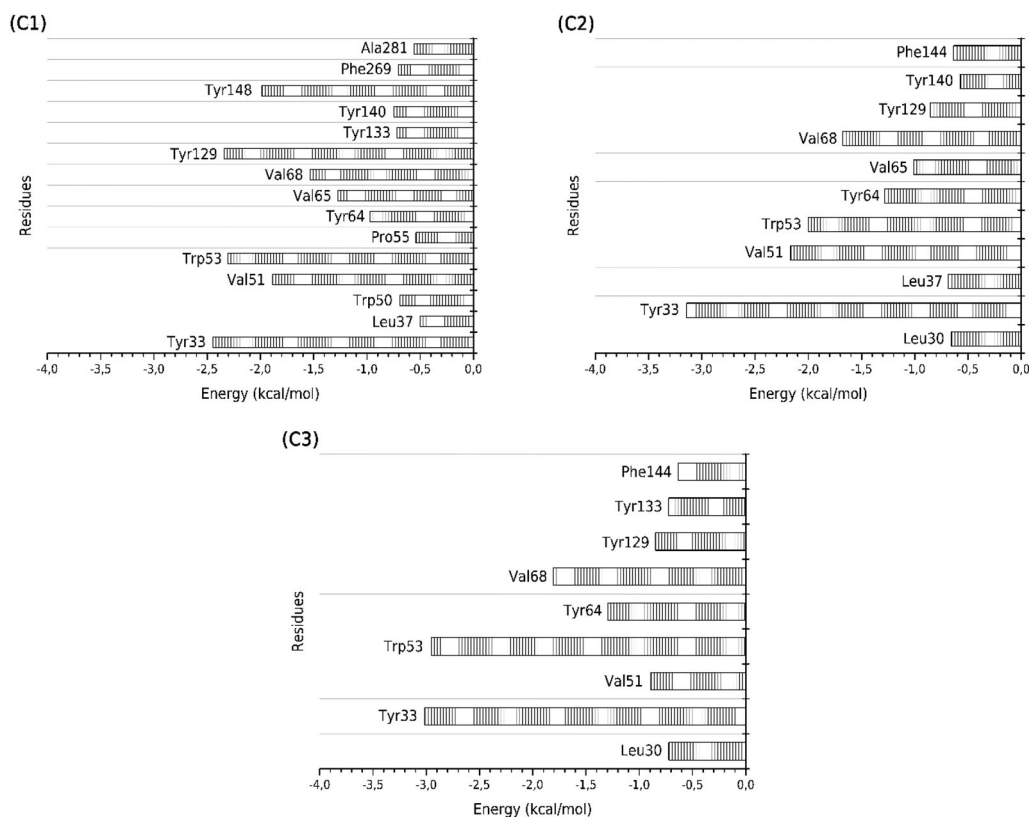


Figure 13. (Continued).

Table 7. Prediction of the binding energy (kcal/mol) of the compounds used as control as well as the new potential inhibitors here proposed.

Receptor	Ligand	Terms					
		ΔE_{vdW}	ΔE_{ele}	ΔG_{GB}	ΔG_{NP}	ΔG_{solv}	ΔG_{bind}
Human AChE	GNT (control)	-39.66 ± 0.07	-14.70 ± 0.10	27.80 ± 0.08	-4.39 ± 0.01	23.41	-30.95 ± 0.09
	15	-46.69 ± 0.10	-11.76 ± 0.14	31.76 ± 0.13	-5.72 ± 0.04	26.04	-32.42 ± 0.12
	5	-51.75 ± 0.09	-1.58 ± 0.09	21.54 ± 0.07	-5.86 ± 0.02	15.68	-37.66 ± 0.19
Insect AChE	I40 (control)	-50.35 ± 0.13	-16.35 ± 0.18	36.69 ± 0.03	-5.21 ± 0.05	31.48	-35.22 ± 0.27
	4	-46.15 ± 0.10	-14.22 ± 0.14	33.28 ± 0.09	-5.38 ± 0.03	27.9	-32.47 ± 0.11
	11	-52.61 ± 0.11	-20.82 ± 0.23	39.75 ± 0.17	-6.14 ± 0.02	33.61	-39.82 ± 0.13
<i>Aedes aegypti</i> JH	JHIII (control)	-48.38 ± 0.11	-18.07 ± 0.10	25.01 ± 0.04	-6.58 ± 0.01	18.43	-48.02 ± 0.11
	15	-52.51 ± 0.13	-11.42 ± 0.09	25.67 ± 0.06	-6.74 ± 0.01	18.93	-45.01 ± 0.11
	16	-44.64 ± 0.09	-9.35 ± 0.09	21.53 ± 0.05	-5.78 ± 0.01	15.75	-38.24 ± 0.09

ΔE_{vdW} , contributions by van der Waals interactions; ΔE_{ele} , electrostatic energy; ΔG_{GB} , polar solvation energy; ΔG_{NP} , nonpolar solvation energy; ΔG_{solv} , desolvation free energy ($\Delta G_{solv} = \Delta G_{GB} + \Delta G_{nonpol}$); ΔG_{bind} , binding affinity.

variations in the conformations of the molecule were observed.

From 0 to 50 ns, the mean RMSD value was 0.76 Å after conformational variation, i.e. from 51 ns the mean RMSD value was ~ 2.03 Å. The difference in these values was 1.27 Å. This conformational variation occurred because the ligand showed a small change in the space occupied at the enzyme active site, as illustrated in Figure 11. However, after conformational change the molecule remained bound to the enzyme active site and interacting with key amino acids for protein inhibition, as can be observed in the results of energy free from decomposition by residue. Thus, it can be concluded that the conformational modification was not able to impair the inhibitor action and was not able to cause drastic losses in its activity, since this ligand exhibited binding free energy value close to that obtained for the crystallographic inhibitor used as a positive control.

The new inhibitors MCULE-8839595892 and MCULE-2164314832 of the juvenile *A. aegypti* hormone were stable at 40 and 10 ns, respectively. Both remained at the binding site until the end of the simulation and were able to satisfactorily inhibit the target protein, as can be seen by our binding free energy results obtained using the MM/GBSA approach.

The flexibility of the receptor backbone was investigated along the MD trajectory by establishing complexes with the compounds used as control and with the proposed new inhibitors. To plot the root-mean-square fluctuations (RMSF) vs the time of molecular dynamics the $C\alpha$ atoms of proteins were used. In Figure 12, it is possible to visualize the fluctuation of the $C\alpha$ of the protein backbone.

The RMSF profile of human AChE (Figure 12A) exhibited flexibility in similar regions of the complexes formed along the time. The greatest fluctuations were observed in the

intervals of 254–279 and 479–504. Residues in the range of 254–275 form a region of the protein comprising two loops intercalated by an alpha helix. Residues from 479 to 504 form a large loop region. These two regions are exposed to the solvent and the loops are structurally more flexible regions of the protein. The other parts of the receiver demonstrated similar flexibility in their structure in the three systems formed, with no major discrepancies.

The *D. melanogaster* AChE systems showed large fluctuations in the residues from 100 to 150. To investigate this region, we divided the interval into two parts, the first consisting of the residues from 100 to 125 and the second from the residues from 126 to 150. The first interval forms a loop region that is exposed to the solvent and exhibits great variation in its dynamics of movement.

The second interval forms a beta sheet region, close to the binding site of the proteins, and a loop that will connect to the loop formed by the first residue range. The lower fluctuation in the RMSF plot of the second range was observed for the system formed with the inhibitor Maybridge3_002654, and this occurred because that molecule established hydrophobic interactions with the residues of that portion of the protein, consequently keeping that portion of the structure more stable and less flexible.

There were no drastic changes in the backbone fluctuation of juvenile Hormone protein in the three systems formed. This may occur because the ligands have similar molecular volumes and settle at the binding site by establishing sufficient intermolecular interactions to remain coupled in the protein cavity.

Molecular interactions in the binding pocket

The values of the binding energies obtained using the MM/GBSA methodology were decomposed to obtain the values of the interaction energies of each residue of the active/receptor site of the protein with the complexed inhibitors. We used this approach to investigate the interactions of the compounds obtained by virtual screening and to compare these interactions with those performed between the enzyme and the control compounds.

Figure 13 shows the amino acids that established important interactions with the inhibitors, on each complex formed. In general, the interaction pattern of the compounds obtained by virtual screening was similar to the interaction pattern of the compounds used as control, with some differences. The similarity in the pattern of interaction of standard and control compounds demonstrates that the proposed novel inhibitors are able to interact effectively with their respective targets as they establish interactions with residues of the protein active sites that are critical for enzymatic inhibition.

The human AChE binding cavity has different subsites. His447 is located in a deep bonding well. Similarly, to the control compound, the new proposed inhibitors were able to interact with this residue that is very important for the enzymatic inhibition. The GNT, MCULE-8839595892 and Maybridge4_001571 molecules also interact with Gly121,

which make up the oxyanion slit of the protein. These inhibitors were also able to interact with another enzyme, by establishing critical interactions with Tyr337 from the anion site.

The MCULE-8839595892 and Maybridge4_001571 inhibitors achieved interactions that the control compound was unable to establish. These interactions were established between the molecule MCULE-8839595892 and the residues Gly120, Tyr124, Phe338, Tyr341, while for the molecule Maybridge4_001571, the residues were Asp74, Tyr119, Gly126, Glu202, Phe338, Tyr341 and Ile451.

The novel compounds with potential activity against the *D. melanogaster* AChE protein have a larger molecular size than the control compound I40. As a consequence, they were able to take up more space from the enzyme binding pocket and achieved interactions with more residues of the binding site. This can be seen considering the larger number of residues that interact with the new compounds by comparing the spectrum of interactions shown in Figure 3.

The interactions established by I40, identified in the crystallographic structure, were maintained. These interactions were with aromatic side chain amino acids, such as Tyr71, Trp83, Trp84, Tyr370 and Tyr374.

The interactions reported by the novel compounds Maybridge3_002654 and Maybridge2_000711 also were with aromatic side-chain amino acids. The molecule Maybridge3_002654 preserved the interactions observed with the docking studies performed with Tyr71, Trp83 and Tyr370. The molecule Maybridge2_000711 preserved the interactions with residues Trp83, Tyr370, Phe371 and Tyr374. Because these compounds have aromatic groupings in their structures, the interactions with the amino acids here observed were mostly hydrophobic and π - π stacking.

The novel JHIII inhibitors showed interactions with several important residues of the protein binding site. The interactions of the molecule MCULE-8839595892 with Tyr33, Val51, Trp53, Tyr64 and Val68 are outstanding. These interactions were observed and discussed in the molecular docking studies here performed and they were also maintained during the molecular dynamic's simulations, which demonstrate that these interactions are critical to the activity of that molecule to inhibit the target protein. The molecule MCULE-2164314832 also preserved several interactions observed in the docking studies. These interactions were with the apolar side chain of Val51 and Val68, as well as with the residues Tyr33, Trp53 and Tyr129.

Binding energy and its components

Using the MM/GBSA approach, we obtained an estimate of the binding energy for all the systems here investigated. In addition, we obtained the values of the free energy components that allowed us to analyse the nature of the chemical interactions that were favourable for the formation of the enzyme–ligand complexes, and the values obtained are summarized in Table 7.

The terms of the mechanical energy and the molecular gas phase were the main responsible for the formation of

the complexes. Thus, van der Waals (ΔE_{vdW}) show the most contribution to the drug-receptor interaction, and secondly the electrostatic contributions (ΔE_{ele}), also favouring the interaction protein–ligand.

The desolvation free energy (ΔG_{solv}) was unfavourable for the systems due to the strong contribution of the polar term (ΔG_{GB}) to the non-interaction of the ligands with the binding site. The non-polar contributions (ΔG_{NP}) were polar opposites, ie ΔG_{NP} favoured the binding of the compounds; however, it was not enough to counterbalance the polar term and makes the energy free of solvation favourable to the establishment of the systems. The binding affinity values (ΔG_{bind}) were all negative, demonstrating that the interaction of the molecules is favourable for the formation of all systems.

Conclusions

The continuous growth of the world population, the great competition between man and insect for the same food, the transmission of diseases and the hospital infection having as vectors the insects, and the adaptation to the existing insecticides by some insects, the development of new insecticides. Mechanism of biological action for the insecticidal effect is still little investigated and research is progressing towards its elucidation, since the studies involving insecticidal research report the performance of the CNS, causing paralysis and, finally, death.

Studies related to the use of receptors that help elucidate the mechanism of action of the insecticidal activity are the key to design molecules that effectively bind to the protein active site, inactivating enzymes, such as acetylcholinesterase which is activated in the CNS to decrease the concentration of acetylcholine in the synaptic cleft. It was not known at the present time molecules that have a dual action for insecticidal activity, because they act in the inhibition of the enzyme acetylcholinesterase and in the juvenile hormone. In this way, rational design can offer a new option for the development and synthesis of novel potential insecticides.

The RMSD results for the compounds here proposed by virtual screening demonstrated that the new molecules are able to interact and to remain stable in the active site of their respective targets, in potential. All the new compounds presented binding energy values close to those obtained for the compounds used as control, demonstrating that the molecules proposed in our study are promising inhibitors of the selected targets. According to the results of energy decomposition per residue, the new inhibitors have an interaction profile similar to those exhibited by the control compounds. Thus, novel ligands are capable of interacting with amino acids that are critical for enzymatic interaction and inhibition.

Molecules **4**, **5**, **11**, **15** and **16** show a good profile for the inhibition of the acetylcholinesterase enzyme and the juvenile hormone, in potential, since the interactions established with the respective proteins were similar to the controls (I40, GNT and pyriproxyfen) used, according the docking studies here performed. The molecules exhibit binding affinity and free energy values with greater stability in the active site compared to the control groups

Disclosure statement

The authors declare no conflict of interest.

Funding

The authors thank Federal University of Amapá, Graduate Program in Biotechnology and Biodiversity-Network BIONORTE, Coordenação de Aperfeiçoamento de Pessoal de Nível Superior (CAPES) and Conselho Nacional de Desenvolvimento Científico e Tecnológico (CNPq) for funding in the publication of this article.

ORCID

Ryan S. Ramos  <http://orcid.org/0000-0003-1802-1320>

References

- Andersen, R. A., Enomoto, M., Miller, E. C., & Miller, J. A. (1964). Carcinogenesis and inhibition of the Walker 256 tumor in the rat by trans-4-acetylaminostilbene, its N-hydroxy metabolite, and related compounds. *Cancer Research*, *24*, 128–143.
- Andrighetti, M. T. M., Cerone, F., Rigueti, M., Galvani, K. C., & Macoris, M. L. G. (2008). Effect of pyriproxyfen in *Aedes aegypti* populations with different levels of susceptibility to the organophosphate temephos. *Dengue Bulletin*, *32*, 186–198.
- Angel, A., Angel, B., Yadav, K., Sharma, N., Joshi, V., Thanvi, I., & Thanvi, S. (2017). Age of initial cohort of dengue patients could explain the origin of disease outbreak in a setting: A case control study in Rajasthan, India. *VirusDisease*, *28*(2), 205–208. doi:10.1007/s13337-017-0377-5
- Areiza, M. (2018). *Regulation of juvenile hormone synthesis by 20-hydroxyecdysone in the yellow-fever mosquito, Aedes aegypti* (PhD Thesis). Florida International University, Miami, FL.
- Banerjee, P., Dehnbostel, F. O., & Preissner, R. (2018). Prediction is a balancing act: Importance of sampling methods to balance sensitivity and specificity of predictive models based on imbalanced chemical data sets. *Frontiers in Chemistry*, *6*, 362. doi:10.3389/fchem.2018.00362
- Banerjee, P., Eckert, A. O., Schrey, A. K., & Preissner, R. (2018). ProTox-II: A webserver for the prediction of toxicity of chemicals. *Nucleic Acids Research*, *46*(W1), W257–W263. doi:10.1093/nar/gky318
- Bardiot, D., Koukni, M., Smets, W., Carlens, G., Kaptein, S., Dallmeier, K., ... Marchand, A. (2018). Discovery of indole derivatives as novel and potent dengue virus inhibitors. *Journal of Medicinal Chemistry*, *61*(18), 8390–8401. doi:10.1021/acs.jmedchem.8b00913
- Barratt, M. D., & Basketter, D. A. (1992). Possible origin of the skin sensitisation potential of isoeugenol and related compounds. (I) Preliminary studies of potential reaction mechanisms. *Contact Dermatitis*, *27*(2), 98–104. doi:10.1111/j.1600-0536.1992.tb05217.x
- Basketter, D. A., Flyvholm, M. A., & Menne, T. (1999). Classification criteria for skin-sensitizing chemicals: A commentary. *Contact Dermatitis*, *40*(4), 175–182. doi:10.1111/j.1600-0536.1999.tb06029.x
- Behnam, M. A. M., Graf, D., Bartenschlager, R., Zlotos, D. P., & Klein, C. D. (2015). Discovery of nanomolar dengue and west nile virus protease inhibitors containing a 4-benzyloxyphenylglycine residue. *Journal of Medicinal Chemistry*, *58*(23), 9354–9370. doi:10.1021/acs.jmedchem.5b01441
- Behnam, M. A., Nitsche, C., Boldescu, V., & Klein, C. D. (2016). The medicinal chemistry of dengue virus. *Journal of Medicinal Chemistry*, *59*(12), 5622–5649. doi:10.1021/acs.jmedchem.5b01653
- Biscarini, L. (2000). Non-steroidal anti-inflammatory drugs. *Meyler's side effects of drugs* (pp. 246–309). 10.1016/B978-0-444-53717-1.01165-3
- Blenau, W., Rademacher, E., & Baumann, A. (2012). Plant essential oils and formamidines as insecticides/acaricides: What are the molecular targets? *Apidologie*, *43*(3), 334–347. doi:10.1007/s13592-011-0108-7

- Braga, I. A., & Valle, D. (2007). *Aedes aegypti*: Inseticidas, mecanismos de ação e resistência. *Epidemiologia e Serviços de Saúde*, 16, 279–293. doi:10.5123/S1679-49742007000400006
- Budryn, G., Pałecz, B., Rachwał-Rosiak, D., Oracz, J., Zaczyńska, D., Belica, S., ... Pérez-Sánchez, H. (2015). Effect of inclusion of hydroxycinnamic and chlorogenic acids from green coffee bean in β -cyclodextrin on their interactions with whey, egg white and soy protein isolates. *Food Chemistry*, 168, 276–287. doi:10.1016/j.foodchem.2014.07.056
- Burkert, U., & Allinger, N. L. (1982). *Molecular mechanics*. ACS monograph 177. Washington, DC: American Chemical Society.
- Cavalcanti, L. P. G., Freitas, A. R. R., Brasil, P., & Cunha, R. V. (2017). Surveillance of deaths caused by arboviruses in Brazil: From dengue to chikungunya. *Memórias Do Instituto Oswaldo Cruz*, 112(8), 583–585. doi:10.1590/0074-02760160537
- Cheung, J., Rudolph, M. J., Burshteyn, F., Cassidy, M. S., Gary, E. N., Love, J., ... Height, J. J. (2012). Structures of human acetylcholinesterase in complex with pharmacologically important ligands. *Journal of Medicinal Chemistry*, 55(22), 10282–10286. doi:10.1021/jm300871x
- Citro, V., Peña-García, J., den-Haan, H., Pérez-Sánchez, H., Del Prete, R., Liguori, L., ... Andreotti, G. (2016). Identification of an allosteric binding site on human lysosomal alpha-galactosidase opens the way to new pharmacological chaperones for Fabry disease. *PLoS One*, 11(10), e0165463. doi:10.1371/journal.pone.0165463
- Collado-González, M., Montalbán, M. G., Peña-García, J., Pérez-Sánchez, H., Villora, G., & Diaz Baños, F. G. (2017). Chitosan as stabilizing agent for negatively charged nanoparticles. *Carbohydrate Polymers*, 161, 63–70. doi:10.1016/j.carbpol.2016.12.043
- Cornell, W. D., Cieplak, P., Bayly, C. I., & Kollman, P. A. (1993). Application of RESP charges to calculate conformational energies, hydrogen bond energies, and free energies of solvation. *Journal of the American Chemical Society*, 115(21), 9620–9631. doi:10.1021/ja00074a030
- Coscollà, C., Vicent, Y., Martí, P., & Pastor, A. (2008). Analysis of currently used pesticides in fine airborne particulate matter (PM 2.5) by pressurized liquid extraction and liquid chromatography–tandem mass spectrometry. *Journal of Chromatography A*, 1200(2), 100–107. doi:10.1016/j.chroma.2008.05.075
- Costa, J. S., Costa, K. L., Cruz, J. V., Ramos, R. S., Silva, L. B., Brasil, D. S. B., ... Macêdo, W. J. C. (2018). Virtual screening and statistical analysis in the design of new caffeine analogues molecules with potential epithelial anticancer activity. *Current Pharmaceutical Design*, 23, 1–19.
- Costa, V. G., Ferreira, E. F. B., da S. Ramos, R., da Silva, L. B., de Sá, E. M. F., da Silva, A. K. P., ... dos Santos, C. B. R. (2019). Hierarchical virtual screening of potential insecticides inhibitors of acetylcholinesterase and juvenile hormone from temephos. *Pharmaceuticals*, 12(2), 61. doi:10.3390/ph12020061
- Cronin, M. T. D., & Basketter, D. A. (1994). Multivariate QSAR analysis of a skin sensitization database. *SAR and QSAR in Environmental Research*, 2(3), 159–179. doi:10.1080/10629369408029901
- Cruz, J. N., Costa, K. S., Carvalho, T. A. A., & Alencar, N. A. N. (2019). Measuring the structural impact of mutations on cytochrome P450 21A2, the major steroid 21-hydroxylase related to congenital adrenal hyperplasia. *Journal of Biomolecular Structure and Dynamics*, 1–17. doi:10.1080/07391102.2019.1607560
- Dalvie, D. K., Kalgutkar, A. S., Khojasteh-Bakht, S. C., Obach, R. S., & O'Donnell, J. P. (2002). Biotransformation reactions of five-membered aromatic heterocyclic rings. *Chemical Research in Toxicology*, 15(3), 269–299. doi:10.1021/tx015574b
- Darden, T., York, D., & Pedersen, L. (1993). Particle mesh Ewald: An $N \cdot \log(N)$ method for Ewald sums in large systems. *Journal of Chemical Physics*, 98(12), 10089–10092. doi:10.1063/1.464397
- Dengue: Guidelines for diagnosis, treatment, prevention and control. (2009). New ed. Geneva: World Health Organization.
- Dolinsky, T. J., Nielsen, J. E., McCammon, J. A., & Baker, N. A. (2004). PDB 2PQR: An automated pipeline for the setup of Poisson-Boltzmann electrostatics calculations. *Nucleic Acids Research*, 32(Web Server), W665–W667. doi:10.1093/nar/gkh381
- Drwal, M. N., Banerjee, P., Dunkel, M., Wettig, M. R., & Preissner, R. (2014). ProTox: A web server for the *in silico* prediction of rodent oral toxicity. *Nucleic Acids Research*, 42(W1), W53–W58. doi:10.1093/nar/gku401
- Engdahl, C., Knutsson, S., Fredriksson, S. Å., Linusson, A., Bucht, G., & Ekström, F. (2015). Acetylcholinesterases from the disease vectors *Aedes aegypti* and *Anopheles gambiae*: Functional characterization and comparisons with vertebrate orthologues. *PLoS One*, 10(10), e0138598. doi:10.1371/journal.pone.0138598
- Ferreira, J. V., Chaves, G. A., Marino, B. L. B., Sousa, K. P. A., Souza, L. R., Brito, M. F. B., ... Hage-Melim, L. I. S. (2017). Cannabinoid type 1 receptor (CB1) bioligand with therapeutic potential for withdrawal syndrome in chemical dependents *Cannabis sativa*. *ChemMedChem*, 12(16), 1408–1416. doi:10.1002/cmdc.201700129
- Fournier, D., Muterio, A., Pralavorio, M., & Bride, J. M. (1993). *Drosophila* acetylcholinesterase: Mechanisms of resistance to organophosphates. *Chemico-Biological Interactions*, 87(1–3), 233–238. doi:10.1016/0009-2797(93)90047-3
- Frisch, M. J., Trucks, G. W., Schlegel, H. B., Scuseria, G. E., Robb, M. A., Cheeseman, J. R., ... Izmaylov, J. L. (2016). Gaussian 16 Revision B.01.
- Gaddaguti, V., Rao, T. V., & Rao, A. P. (2016). Potential mosquito repellent compounds of *Ocimum* species against 3N7H and 3Q8I of *Anopheles gambiae*. *3 Biotech*, 6(1), 26. doi:10.1007/s13205-015-0346-x
- Gnagey, A. L., Forte, M., & Rosenberry, T. L. (1987). Isolation and characterization of acetylcholinesterase from *Drosophila*. *Journal of Biological Chemistry*, 262(27), 13290–13298.
- Goel, R. K., Singh, D., Lagunin, A., & Poroikov, V. (2011). PASS-assisted exploration of new therapeutic potential of natural products. *Medicinal Chemistry Research*, 20(9), 1509–1514. doi:10.1007/s00044-010-9398-y
- Gohlke, H., Kiel, C., & Case, D. A. (2003). Insights into protein–protein binding by binding free energy calculation and free energy decomposition for the Ras–Raf and Ras–RalGDS complexes. *Journal of Molecular Biology*, 330(4), 891–913. doi:10.1016/S0022-2836(03)00610-7
- Gowtham, U., Jayakanthan, M. D., & Sundar, S. (2008). Molecular docking studies of dithionitrobenzoic acid and its related compounds to protein disulfide isomerase: Computational screening of inhibitors to HIV-1 entry. *BMC Bioinformatics*, 9, S14. doi:10.1186/1471-2105-9-S12-S14
- Harburguer, L. V., Seccacini, E., Masuh, H., González Audino, P., Zerba, E., & Licastro, S. (2009). Thermal behaviour and biological activity against *Aedes aegypti* (Diptera: Culicidae) of permethrin and pyriproxyfen in a smoke-generating formulation. *Pest Management Science*, 65(11), 1208–1214. doi:10.1002/ps.1811
- Harel, M., Kryger, G., Rosenberry, T. L., Mallender, W. D., Lewis, T., Fletcher, R. J., ... Sussman, J. L. (2000). Three-dimensional structures of *Drosophila melanogaster* acetylcholinesterase and of its complexes with two potent inhibitors. *Protein Science*, 9(6), 1063–1072. doi:10.1110/ps.9.6.1063
- Harwood, J. F., Helme, W. L., Turnwall, B. B., Justice, K. D., Muhammed Farooq, M., & Richardson, A. G. (2016). Controlling *Aedes aegypti* in cryptic environments with manually carried ultra-low volume and mist blower pesticide applications. *Journal of the American Mosquito Control Association*, 32(3), 217–223. doi:10.2987/16-6553.1
- Hawkins, P. C. D., & Nicholls, A. (2012). Conformer generation with OMEGA: Learning from the data set and the analysis of failures. *Journal of Chemical Information and Modeling*, 52(11), 2919–2936. doi:10.1021/ci300314k
- Hay, S. I., George, D. B., Wint, G. R. W., Hoen, A. G., Brownstein, J. S., Bhatt, S., ... Simmons, C. P. (2013). The global distribution and burden of dengue. *Nature*, 496, 504–507. doi:10.1038/nature12060
- Hevener, K. E., Zhao, W., Ball, D. M., Babaoglu, K., Qi, J., White, S. W., & Lee, R. E. (2009). Validation of molecular docking softwares for virtual screening against dihydropteroate synthase. *Journal of Chemical Information and Modeling*, 49(2), 444–460. doi:10.1021/ci800293n
- Holder, J. W. (1999). Nitrobenzene carcinogenicity in animals and human hazard evaluation. *Toxicology and Industrial Health*, 15, 445–457.
- Inoue, M., Akimoto, T., Saito, O., Ando, Y., Muto, S., & Kusano, E. (2008). Successful relatively low-dose corticosteroid therapy for diclofenac-induced acute interstitial nephritis with severe renal failure. *Clinical and Experimental Nephrology*, 12(4), 296–299. doi:10.1007/s10157-008-0039-4
- Iswardy, E., Tsai, T.-C., Cheng, I.-F., Ho, T.-C., Perng, G. C., & Chang, H.-C. (2017). A bead-based immunofluorescence-assay on a microfluidic dielectrophoresis platform for rapid dengue virus detection.

- Biosensors and Bioelectronics*, 95, 174–180. doi:10.1016/j.bios.2017.05.038
- Itoh, M. (1982). Sensitization potency of some phenolic compounds. *The Journal of Dermatology*, 9(3), 223–233. doi:10.1111/j.1346-8138.1982.tb02629.x
- Izaguirre, J. A., Catarello, D. P., Wozniak, J. M., & Skeel, R. D. (2001). Langevin stabilization of molecular dynamics. *Journal of Chemical Physics*, 114(5), 2090–2098. doi:10.1063/1.1332996
- Jalota, R., & Freston, J. W. (1974). Severe intrahepatic cholestasis due to thiabendazole. *The American Journal of Tropical Medicine and Hygiene*, 23(4), 676–678. doi:10.4269/ajtmh.1974.23.676
- Jorgensen, W. L., Chandrasekhar, J., Madura, J. D., Impey, R. W., & Klein, M. L. (1983). Comparison of simple potential functions for simulating liquid water. *Journal of Chemical Physics*, 79(2), 926–935. doi:10.1063/1.445869
- Kalgutkar, A. S., Gardner, I., Obach, R. S., Shaffer, C. L., Callegari, E., Henne, K. R., ... Harriman, S. P. (2005). A comprehensive listing of bioactivation pathways of organic functional groups. *Current Drug Metabolism*, 6(3), 161–225. doi:10.2174/1389200054021799
- Kang, G., Kim, J., Park, H., & Kim, T. H. (2015). Crystal structure of pyriproxyfen. *Acta Crystallographica*, 71, 588.
- Kayser, D., & Schlede, E. (2001). *Chemikalien und Kontaktallergie: Eine Bewertende Zusammenstellung, Chemikalien und Kontaktallergie: Eine Bewertende Zusammenstellung*. Munich: Urban & Vogel Medien und Medizin Verlagsgesellschaft.
- Kim, I. H., Pham, V., Jablonka, W., Goodman, W. G., Ribeiro, J. M. C., & Andersen, J. F. (2017). A mosquito hemolymph odorant-binding protein Family member specifically binds juvenile hormone. *Journal of Biological Chemistry*, 292(37), 15329–15339. doi:10.1074/jbc.M117.802009
- Kirchmair, J., Göller, A. H., Lang, D., Kunze, J., Testa, B., Wilson, I. D., ... Schneider, G. (2015). Predicting drug metabolism: Experiment and/or computation? *Nature Reviews Drug Discovery*, 14(6), 387–404. doi:10.1038/nrd4581
- Kobayashi, H., Suzuki, T., Akahori, F., & Satoh, T. (2011). Receptors: Brain regional heterogeneity. In: T. Satoh & R. C. Gupta (Eds.), *Anticholinesterase Pesticides: Metabolism, Neurotoxicity, and Epidemiology* (Vol. 3, pp. 3–18).
- Kollman, P. A., Massova, I., Reyes, C., Kuhn, B., Huo, S., Chong, L., ... Cheatham, T. E. (2000). Calculating structures and free energies of complex molecules: Combining molecular mechanics and continuum models. *Accounts of Chemical Research*, 33(12), 889–897. doi:10.1021/ar000033j
- Kovacic, P., & Jacintho, J. D. (2001). Mechanisms of carcinogenesis: Focus on oxidative stress and electron transfer. *Current Medicinal Chemistry*, 8(7), 773–796. doi:10.2174/0929867013373084
- Kroupova, A., Ivaşcu, A., Reimão-Pinto, M. M., Ameres, S. L., & Jinek, M. (2019). Structural basis for acceptor RNA substrate selectivity of the 3 terminal uridylyl transferase Tailor. *Nucleic Acids Research*, 47(2), 1030–1042. doi:10.1093/nar/gky1164
- Leal, E. S., Aucar, M. G., Gebhard, L. G., Iglesias, N. G., Pascual, M. J., Casal, J. J., & Bollini, M. (2017). Discovery of novel dengue virus entry inhibitors via a structure-based approach. *Bioorganic & Medicinal Chemistry Letters*, 27(16), 3851–3855. doi:10.1016/j.bmcl.2017.06.049
- Lhasa Limited. (2007). *Derek Nexus; Versão 10.0.2*. Leeds, UK: Lhasa Limited.
- Lipinski, C. A., Lombardo, F., Dominy, B. W., & Feeney, P. J. (2001). Experimental and computational approaches to estimate solubility and permeability in drug discovery and development settings. *Advanced Drug Delivery Reviews*, 46(1–3), 3–26. doi:10.1016/S0169-409X(00)00129-0
- Maier, J. A., Martinez, C., Kasavajhala, K., Wickstrom, L., Hauser, K. E., & Simmerling, C. (2015). ff14SB: Improving the accuracy of protein side chain and backbone parameters from ff99SB. *Journal of Chemical Theory and Computation*, 11(8), 3696–3713. doi:10.1021/acs.jctc.5b00255
- Martínez-Ballesta, M., Del, C., Pérez-Sánchez, H., Moreno, D. A., & Carvajal, M. (2016). Plant plasma membrane aquaporins in natural vesicles as potential stabilizers and carriers of glucosinolates. *Colloids and Surfaces B: Biointerfaces*, 143, 318–326. doi:10.1016/j.colsurfb.2016.03.056
- Meriç, A. (2017). Molecular modelling of 2-iminothiazoles as insecticidal activity. *Bulgarian Chemical Communications*, 49, 5–14.
- Miller, E. C. (1978). Some current perspectives on chemical carcinogenesis in humans and experimental animals: Presidential address. *Cancer Research*, 38(6), 1479–1496.
- Miyazawa, M., Tougo, H., & Ishihara, M. (2001). Inhibition of acetylcholinesterase activity by essential oil from *Citrus paradisi*. *Natural Product Letters*, 15, 205–210.
- Mizutani, T., & Suzuki, K. (1996). Relative hepatotoxicity of 2-(substituted phenyl) thiazoles and substituted thiobenzamides in mice: Evidence for the involvement of thiobenzamides as ring cleavage metabolites in the hepatotoxicity of 2-phenylthiazoles. *Toxicology Letters*, 85(2), 101–105. doi:10.1016/0378-4274(96)03646-6
- Navarro-Fernández, J., Pérez-Sánchez, H., Martínez-Martínez, I., Meliciani, I., Guerrero, J. A., Vicente, V., ... Wenzel, W. (2012). In silico discovery of a compound with nanomolar affinity to antithrombin causing partial activation and increased heparin affinity. *Journal of Medicinal Chemistry*, 55(14), 6403–6412. doi:10.1021/jm300621j
- Naylor, E., Arredouani, A., Vasudevan, S. R., Lewis, A. M., Parkesh, R., Mizote, A., ... Ganesan, A. (2009). Identification of a chemical probe for NAADP by virtual screening. *Nature Chemical Biology*, 5(4), 220–226. doi:10.1038/nchembio.150
- Nitsche, C., Schreier, V. N., Behnam, M. A. M., Kumar, A., Bartenschlager, R., & Klein, C. D. (2013). Thiazolidinone-peptide hybrids as dengue virus protease inhibitors with antiviral activity in cell culture. *Journal of Medicinal Chemistry*, 56(21), 8389–8403. doi:10.1021/jm400828u
- O'Donnell, J. P., Dalvie, D. K., Kalgutkar, A. S., & Obach, R. S. (2003). Mechanism-based inactivation of human recombinant P450 2C9 by the nonsteroidal anti-inflammatory drug suprofen. *Drug Metabolism and Disposition*, 31, 1369–1377. doi:10.1124/dmd.31.11.1369
- Oliveira, M. S., Cruz, J. N., Gomes Silva, S., Costa W, A., Sousa S, H. B., Bezerra, F. W. F., ... Carvalho, R. N. (2019). Phytochemical profile, antioxidant activity, inhibition of acetylcholinesterase and interaction mechanism of the major components of the *Piper divaricatum* essential oil obtained by supercritical CO₂. *The Journal of Supercritical Fluids*, 145, 74–84. doi:10.1016/j.supflu.2018.12.003
- Olmstead, A. W., & Leblanc, G. A. (2003). Insecticidal juvenile hormone analogs stimulate the production of male offspring in the crustacean *Daphnia magna*. *Environmental Health Perspectives*, 111(7), 919–924. doi:10.1289/ehp.5982
- Opdyke, D. L. J. (1979). Fragrance raw materials monographs: Alpha-methylanisalacetone. *Food and Cosmetics Toxicology*, 17(5), 509. doi:10.1016/0015-6264(79)90012-9
- Osman, H., Idris, N. H., Kamarulzaman, E. E., Wahab, H. A., & Hassan, M. Z. (2017). 3,5-Bis(arylidene)-4-piperidones as potential dengue protease inhibitors. *Acta Pharmaceutica Sinica B*, 7(4), 479–484. doi:10.1016/j.apsb.2017.04.009
- Ostetmann, K., Borloz, A., Urbain, A., & Marston, A. (2006). Natural product inhibitors of acetylcholinesterase. *Current Organic Chemistry*, 10, 825–847. doi:10.2174/138527206776894410
- Parvez, M. K., & Parveen, S. (2017). Evolution and emergence of pathogenic viruses: Past, present, and future. *Intervirology*, 60(1–2), 1–7. doi:10.1159/000478729
- Pascoe, M. D., Gordon, G. D., & Temple-Camp, C. R. E. (1986). Tolmetin-induced acute renal failure. A case report. *South African Medical Journal*, 70(4), 232–233.
- Paul, A., Harrington, L. C., & Scott, J. G. (2006). Evaluation of novel insecticides for control of dengue vector *Aedes aegypti* (Diptera: Culicidae). *Journal of Medical Entomology*, 43(1), 55–60. doi:10.1093/jmedent/43.1.55
- Picard, O., Rosmorduc, O., & Cabane, J. (1998). Hepatotoxicity associated with ritonavir. *Annals of Internal Medicine*, 129(8), 670–671. doi:10.7326/0003-4819-129-8-199810150-00026
- Pizova, H., Havelkova, M., Stepankova, S., Bak, A., Kauerova, T., Kozik, V., ... Bobal, P. (2017). Proline-based carbamates as cholinesterase inhibitors. *Molecules*, 22(11), 1969. doi:10.3390/molecules22111969
- Porile, J. L., Bakris, G. L., & Garella, S. (1990). Acute interstitial nephritis with glomerulopathy due to nonsteroidal anti-inflammatory agents: A

- review of its clinical spectrum and effects of steroid therapy. *The Journal of Clinical Pharmacology*, 30(5), 468–475. doi:10.1002/j.1552-4604.1990.tb03487.x
- Ramos, R. S., Costa, J. S., Silva, R. C., da Costa, G. V., Rodrigues, A. B. L., Rabelo, É. M., ... Macêdo, W. J. C. (2019). Identification of potential inhibitors from pyriproxyfen with insecticidal activity by virtual screening. *Pharmaceuticals*, 12(1), 20. doi:10.3390/ph12010020
- Rindings, J. E., Barratt, M. D., & Cary, R. (1996). Computer prediction of possible toxic action from chemical structure, an update of the DEREK system. *Toxicology*, 106, 267–279. doi:10.1016/0300-483X(95)03190-Q
- Ryckaert, J. P., Ryckaert, J. P., Ciccotti, G., & Berendsen, H. J. C. C. (1977). Numerical integration of the Cartesian equations of motion of a system with constraints: Molecular dynamics of n-alkanes. *Journal of Computational Physics*, 23(3), 327–341. doi:10.1016/0021-9991(77)90098-5
- Sáez-Llorens, X., Tricou, V., Yu, D., Rivera, L., Tuboi, S., Garbes, P., ... Wallace, D. (2017). Safety and immunogenicity of one versus two doses of Takeda's tetravalent dengue vaccine in children in Asia and Latin America: Interim results from a phase 2, randomised, placebo-controlled study. *The Lancet Infectious Diseases*, 17(6), 615–625. doi:10.1016/S1473-3099(17)30166-4
- Salomon-Ferrer, R., Case, D. A., & Walker, R. C. (2013). An overview of the Amber biomolecular simulation package. *Wiley Interdisciplinary Reviews: Computational Molecular Science*, 3(2), 198–210. doi:10.1002/wcms.1121
- Sánchez-Linares, I., Pérez-Sánchez, H., Cecilia, J. M., & García, J. M. (2012). High-throughput parallel blind virtual screening using BINDSURF. *BMC Bioinformatics*, 13(Suppl 14), S13. doi:10.1186/1471-2105-13-S14-S13
- Sanderson, D. M., & Earnshaw, C. G. (1991). Computer prediction of possible toxic action from chemical structure; the DEREK system. *Human & Experimental Toxicology*, 10(4), 261–273. doi:10.1177/096032719101000405
- Savelev, S., Okello, E., Perry, N. S. L., Wilkins, R. M., & Perry, E. K. (2003). Synergistic and antagonistic interactions of anticholinesterase terpenoids in *Salvia lavandulaefolia* essential oil. *Pharmacology Biochemistry and Behavior*, 75(3), 661–668. doi:10.1016/S0091-3057(03)00125-4
- Schmitt, H., Altenburger, R., Jastorff, B., & Schuurmann, G. (2000). Quantitative structure-activity analysis of the algae toxicity of nitroaromatic compounds. *Chemical Research in Toxicology*, 13(6), 441–450. doi:10.1021/tx9901635
- Schrödinger. (2011). *QikProp: Rapid ADME predictions of drug candidates; Versão 3.4*. New York, NY: Schrödinger.
- Silva, R. C., Poiani, J. G. C., Ramos, R. S., Costa, J. S., Silva, C. H. T. P., Brasil, D. S. B., & Santos, C. B. R. (2018). Ligand- and structure-based virtual screening from 16-(N, N-diisobutylaminomethyl)-6 α hydroxyvovacapane-7 β ,17 β -lactone compound with potential anti-prostate cancer activity. *Journal of the Serbian Chemical Society*, 83, 1–23.
- Silva, S. G., da Costa, R. A., de Oliveira, M. S., da Cruz, J. N., Figueiredo, P. L. B., Brasil, D. S. B., ... Andrade, E. H. D. A. (2019). Chemical profile of lippia thymoides, evaluation of the acetylcholinesterase inhibitory activity of its essential oil, and molecular docking and molecular dynamics simulations. *PLoS One*, 14(3), e0213393. doi:10.1371/journal.pone.0213393
- Sittivicharpinyo, T., Wonnapijit, P., & Surat, W. (2017). Complete coding sequence of dengue virus serotype 4 isolated from field-caught mosquitoes in Thailand. *Memórias Do Instituto Oswaldo Cruz*, 112(8), 580–582. doi:10.1590/0074-02760170022
- Skandrani, K., Richardet, J. P., Duvoux, C., Cherqui, D., Zafrani, E. S., & Dhumeaux, D. (2008). Hepatic transplantation for severe ductopenia related to ingestion of thiabendazole [French]. *Gastroenterologie Clinique et Biologique*, 21, 623–625.
- Sullivan, J. J., & Goh, K. S. (2008). Environmental fate and properties of pyriproxyfen. *Journal of Pesticide Science*, 33(4), 339–350. doi:10.1584/jpestics.R08-02
- Takahashi, K., Kawazoe, Y., Tada, M., Tada, M., Ito, N., & Okada, M. (1978). Carcinogenicity of 4-nitroquinoline 1-oxide and its possible role in carcinogenesis by 4-nitroquinoline 1-oxide. *Gann*, 69(4), 499–505.
- Testa, B., Balmat, A. L., Long, A., & Judson, P. (2005). Predicting drug metabolism—An evaluation of the expert system METEOR. *Chemistry & Biodiversity*, 2(7), 872–885. doi:10.1002/cbdv.200590064
- Treiber, A., Dansette, P. M., El Amri, H., Girault, J. P., Ginderow, D., Mornon, J. P., & Mansuy, D. (1997). Chemical and biological oxidation of thiophene: Preparation and complete characterization of thiophene S-oxide dimers and evidence for thiophene S-oxide as an intermediate in thiophene metabolism in vivo and in vitro. *Journal of the American Chemical Society*, 119(7), 1565–1571. doi:10.1021/ja962466g
- Vale, A., & Lotti, M. (2015). Organophosphorus and carbamate insecticide poisoning. *Handbook of Clinical Neurology*, 131, 149–168.
- Wang, J., Wang, W., Kollman, P. A., & Case, D. A. (2006). Automatic atom type and bond type perception in molecular mechanical calculations. *Journal of Molecular Graphics and Modelling*, 25(2), 247–260. doi:10.1016/j.jmgl.2005.12.005
- Wang, J., Wolf, R. M., Caldwell, J. W., Kollman, P. A., & Case, D. A. (2004). Development and testing of a general amber force field. *Journal of Computational Chemistry*, 25(9), 1157–1174. doi:10.1002/jcc.20035
- Weigel, L. F., Nitsche, C., Graf, D., Bartenschlager, R., & Klein, C. D. (2015). Phenylalanine and phenylglycine analogues as arginine mimetics in dengue protease inhibitors. *Journal of Medicinal Chemistry*, 58(19), 7719–7733. doi:10.1021/acs.jmedchem.5b00612
- Williams, G. M., & Weisburger, J. H. (1993). In M. O. Amdur, J. Doull, & C. D. Klaassen (Eds.), *Chemical carcinogenesis. Casarett and Doull's toxicology: The basic science of poisons* (4th ed., pp. 127–200). New York, NY: McGraw-Hill.
- World Health Organization. (2009). *The WHO recommended classification of pesticides by hazard and guidelines to classification*. Paris, France: World Health Organization.
- Yamashita, S., Furubayashi, T., Kataoka, M., Sakane, T., Sezaki, H., & Tokuda, H. (2000). Optimized conditions for prediction of intestinal drug permeability using Caco-2 cells. *European Journal of Pharmaceutical Sciences*, 10(3), 195–204. doi:10.1016/S0928-0987(00)00076-2
- Yang, Y., Dong, B., Xu, H., Zheng, X., Heong, K. L., & Lu, Z. (2014). Susceptibility to insecticides and ecological fitness in resistant rice varieties of field *Nilaparvata lugens* Stål population free from insecticides in laboratory. *Rice Science*, 21(3), 181–186. doi:10.1016/S1672-6308(13)60181-X
- Zhang, L., Gao, H., Hansch, C., & Selassie, C. D. (1998). Molecular orbital parameters and comparative QSAR in the analysis of phenol toxicity to leukemia cells. *Journal of the Chemical Society, Perkin Transactions 2*, 2, 2553–2556. doi:10.1039/a801684d